Biotechnology Research and Innovation, 2025, 9(1): e2025002. https://doi.org/10.4322/biori.00022025

Biotechnology Research & Innovation

www.biori.periodikos.com.br

RESEARCH PAPER

Scenedesmus sp. biomass enriched with low-cost polysaccharides to produce hydrogels: a biotechnological approach

Amanda Fonseca Leitzke[a], Diego Serrasol do Amaral[a], Cristina Jansen-Alves[a,b], Carem Perleberg[a], Daisa Hakbart Bonemann[a], Nathalia Stark Pedra[c], Juliane Torchelsen Saraiva[c], Francieli da Silva dos Santos[c], Roselia Spanevello[c], Elessandra da Rosa Zavareze[b], Claudio Martin Pereira de Pereira[a,*]

[a] *Laboratory of Innovation and Solutions in Chemistry, Bioforensics Research Group, Federal University of Pelotas – UFPel, 96160-000, Jardim América, Pelotas, RS, Brazil*
[b] *Laboratory of Biopolymers and Nanotechnology in Food (BioNano), Postgraduate Program in Food Science and Technology, Department of Agroindustrial Science and Technology, Federal University of Pelotas – UFPel, 96160-000, Jardim América, Pelotas, RS, Brazil*
[c] *Postgraduate Program in Biochemistry and Bioprospecting – Neurochemistry, Inflammation and Cancer Laboratory, Center of Chemical, Pharmaceutical and Food Sciences, Federal University of Pelotas – UFPel, University Campus s/n, 96160-000, Jardim América, Pelotas, RS, Brazil*

Highlights

- *Scenedesmus* biomass enriched hydrogels developed for biotechnological use
- Controlled release of phenolic compounds enhances bioactive potential
- Biocompatible hydrogels show strong antioxidant and cell-protective effects

Received 09 April, 2025; Accepted 08 October, 2025.

KEYWORDS
Hydrogel;
Phenolic compounds;
Controlled release;
Cytotoxicity,
Antioxidant.

Abstract: Microalgae of the Scenedesmus genus are recognized for their bioactive compounds and rapid biomass production. This study explores the integration of *Scenedesmus sp.* biomass into hydrogels based on commercial xanthan gum and sodium alginate for controlled release of active substances. Comprehensive characterization revealed a protein content of 4.37%, lipids at 14.4%, and phenolic compounds measuring 0.10 mg GAE/g. Hydrogels demonstrated efficient incorporation and controlled release of bioactive compounds, with release kinetics influenced by the medium. Cytotoxicity assessments showed no adverse effects on L929 fibroblast viability, while reactive oxygen species (ROS) levels were significantly reduced by up to 73.68% for 1% hydrogels. These results highlight the antioxidant potential of the hydrogel for the formulation of bioproducts with controlled release of bioactives, opening new perspectives for innovative applications in cosmetics, nutraceuticals and pharmaceuticals.

*Corresponding author:
E-mail: innovaschem@gmail.com (C. M. P. Pereira).

Graphical Abstract

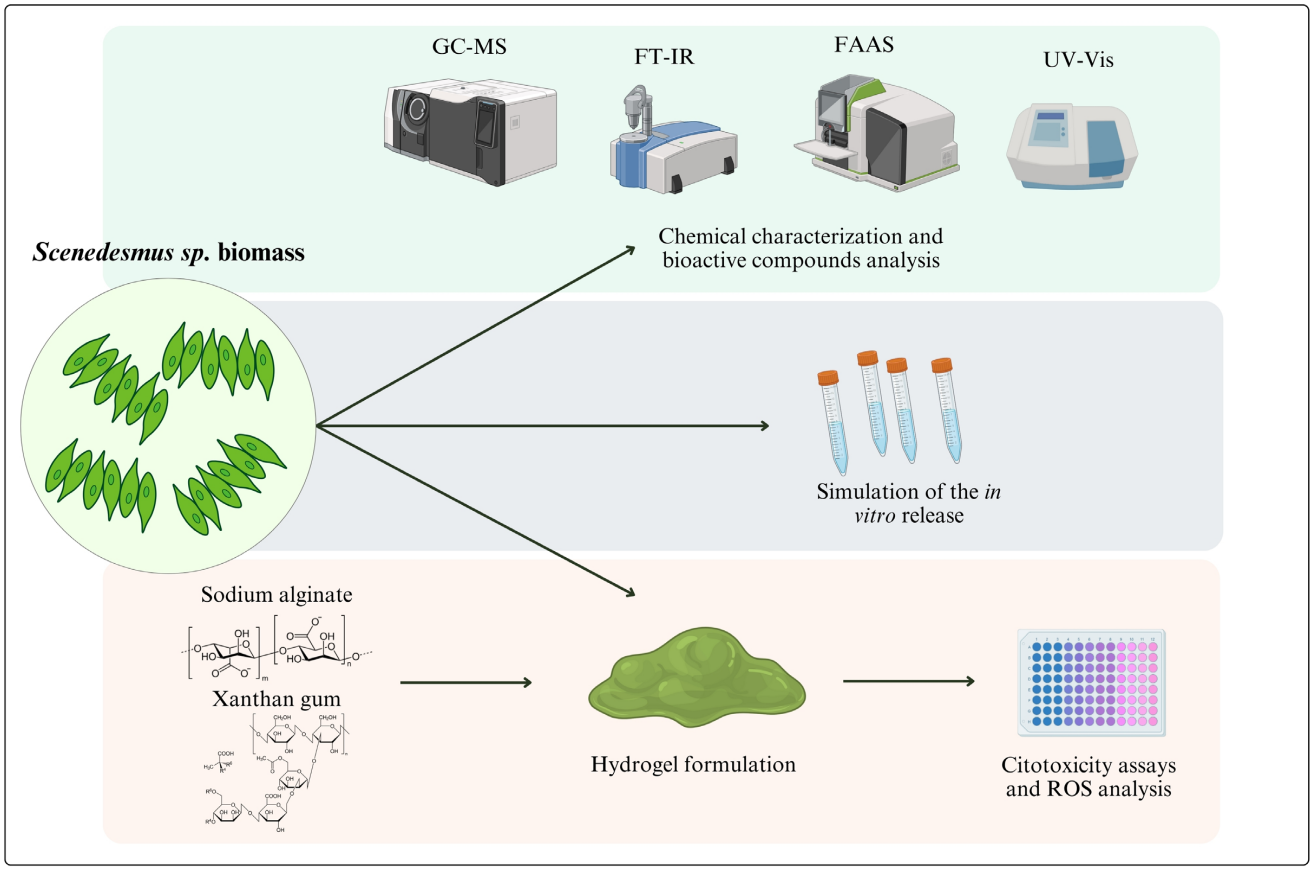

***Scenedesmus sp*. biomass was incorporated into xanthan-alginate hydrogels, creating biocompatible matrices with controlled release of bioactives and strong antioxidant potential for biotechnological applications.**

Introduction

The biotechnological potential of microalgae has begun to be explored on a larger scale in recent years, primarily due to their ability to produce a diverse range of bioactive compounds with a wide range of applications. Their exceptional nutrient assimilation, bioaccumulation efficiency, and high biomass productivity make them a sustainable alternative to conventional raw materials. Unlike traditional resources, microalgae cultivation does not compete for arable land or freshwater, offering unique advantages for the production of bioactive compounds, pigments, and nuttraceuticals (Mendonça et al., 2021; Liu et al., 2022).

Microalgae are an important biomass in industrial applications, including pharmaceuticals, aquaculture, animal feed, and biofertilizers. They are also utilized in environmental biotechnology for purposes such as monitoring environmental pollutants, bioremediation, and conducting bioassays (Rizwan et al., 2018). In addition, microalgae can fix atmospheric CO_2, and grow in diverse environments such as freshwater, wastewater or seawater. When cultivated in wastewater, they consume the nutrients present there, favoring bioremediation and, in parallel, reducing treatment costs (Javed et al., 2019).

Among the microalgae that stand out for their production of bioactive compounds is *Scenedesmus* sp., which belongs to the Sphaeropleales order of the Scenedesmaceae family and is often found in freshwater lakes and rivers (Guiry, 2014). Many species of this genus are being used for various purposes due to their ability to adapt to adverse environmental conditions, their capacity for rapid growth and their ease of cultivation and handling (Ishaq et al., 2016; Mobin & Alam, 2017). *Scenedesmus* sp. is a prolific source of bioactive compounds, including phenolic compounds, carotenoids such as lutein, astaxanthin, and ß-carotene, along with vitamins B, C, and E, polysaccharides, amino acids, and fatty acids (Udayan et al., 2017). Among these, phenolic compounds are highlighted due to their wide-ranging therapeutic applications, particularly their antioxidative and anti-inflammatory properties (Albuquerque et al., 2021). It has been used in different sectors, including pharmaceuticals, food, cosmetics, energy, aquaculture and medicine.

The use of microalgae in the form of food supplements has been addressed (Soltani et al., 2016), as a new source of bioactive compounds with in vitro pharmacological application (Patil & Kaliwal, 2019) and as a source of food and medicines (Sathasivam et al., 2019). Studies show that the bioactive compounds present in microalgae can be better utilized when they are inserted into liposomes, microcapsules, hydrogels or emulsions (Al-Mossawi et al., 2021).

Hydrogels are highly suitable for microalgae immobilization due to their unique properties, such as permeability to gases and nutrients and favorable mechanical characteristics (Kopač et al., 2023). Several microalgal-based hydrogels have been documented in the literature. For instance, *Chlorella vulgaris* cells have been immobilized in an alginate network to create an algae/alginate-based living electrode (Al-Mossawi et al., 2021). Similarly, Chen et al. (2021) developed hydrogels composed of symbiotic algae-bacteria systems to neutralize highly toxic hydroxyl radicals and reduce inflammation, demonstrating excellent biocompatibility and promoting cell proliferation, thus facilitating wound healing.

The study of polymers that enhance the properties of microalgae-derived hydrogels, particularly for biomedical, pharmaceutical, and food applications, remains an area of significant interest. In this regard, the use of xanthan gum and alginate in hydrogel production is well justified due to their favorable physicochemical properties and biocompatibility (Furtado et al., 2022). Xanthan gum serves as an emulsifying and stabilizing agent in various consumer products, including lotions, shampoos, deodorants, facial creams, and moisturizers. These applications are further supported by its renewable origin and non-toxic nature, making it environmentally and biologically safe (Freitas et al., 2015). Similarly, alginate, a naturally occurring polysaccharide derived from brown algae, is widely utilized in the food industry to modify product rheology (thickening), enhance water-binding capacity, stabilize emulsions, and form films (Ching et al., 2017). Despite extensive research on alginate-based hydrogels, no studies have yet reported the formulation of sodium alginate and xanthan gum hydrogels incorporating the microalgae *Scenedesmus* sp. In this context, the present study aimed to evaluate the potential of biocompound release from hydrogels formulated with commercial xanthan gum and sodium alginate, incorporating *Scenedesmus* sp. biomass. The hydrogels were subsequently analyzed for their UV-Visible absorption properties and the controlled release of phenolic compounds in a simulated digestion medium. Additionally, the *Scenedesmus* sp. biomass was characterized in terms of protein, lipid, fiber, ash, and moisture content, along with its bioactive compound profile, metal composition, and fatty acid content.

Material and methods

Cultivation of the microalgae *Scenedesmus* sp.

The *Scenedesmus* sp. microalgae (Figure 1) was sourced from Startup Terramares, Rio Grande, RS, Brazil. Cultivation was carried out in 250 L photobioreactors using Wright's Cryptophyte (WC) culture medium (Guillard & Lorenzen, 1972) with a stable pH range of 7–8. The culture was maintained at 24 ± 2 °C, with aeration provided by compressed air injection. Illumination was achieved using 40 W fluorescent lamps, following a 12-hour light/dark photoperiod to ensure optimal growth conditions.

Material

The materials used for the hydrogel were: xanthan gum (Analitic Insumos, CAS: 11138-66-2) and sodium alginate (Dinâmica, CAS: 9005-38-3). The reagents used were P.A. grade ethyl alcohol (Merck, CAS: 64-17-5) and HPLC grade n-hexane (Supelco, CAS 110-54-3), and the derivatizer boron trifluoride (BF_3) (Sigma-Aldrich, CAS 13319-75-0). All the other chemicals used were of P.A. grade.

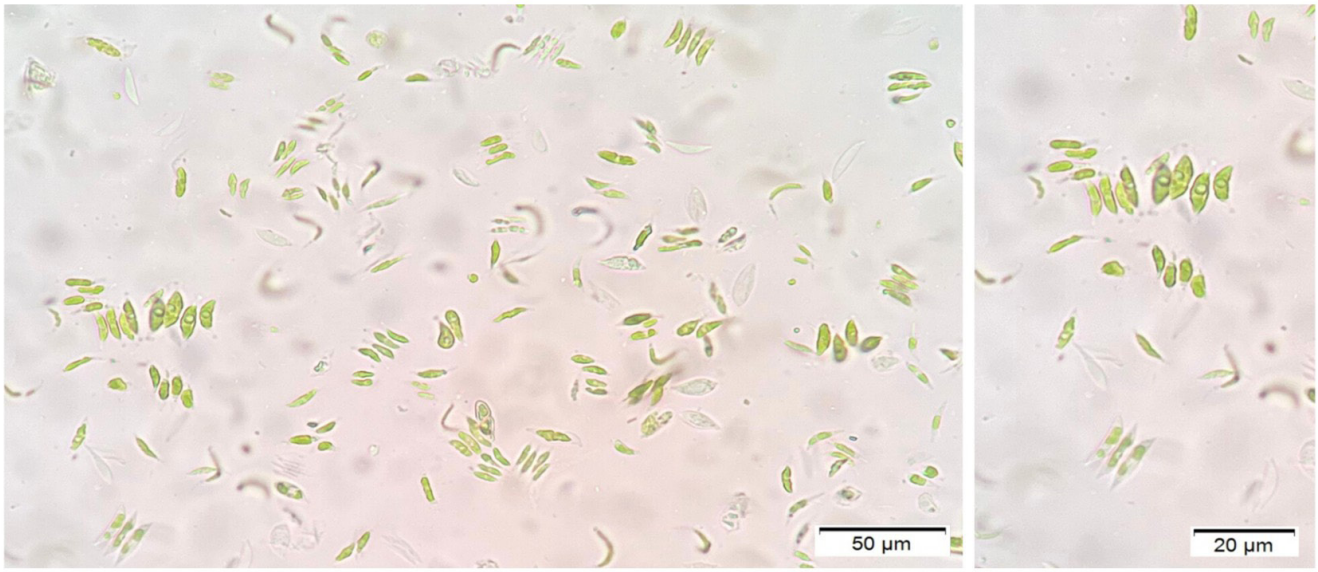

Figure 1. Microalgae *Scenedemus sp*. under an optical microscope.

Chemical analysis

Moisture

Moisture analysis of the microalgae was carried out in an oven at 105 ºC for up to 6 hours. Moisture was calculated using gravimetry (Association of Official Agricultural Chemists, 2016).

Protein

The protein content was determined using the digital digestion block microsystem (Kjeldahl), where 300 mg of the microalgae were transferred to the Kjeldahl tube where 2 g of catalytic mixture and 10 mL of concentrated sulfuric acid were added (Association of Official Agricultural Chemists, 2016). The samples were digested at 350 ºC for 4 hours until they showed a light green to white color. Afterwards, 50 mL of distilled water was added to the Kjeldahl tube. For distillation, 40 mL of 50% (v/v) sodium hydroxide was used. The condenser remained immersed in a 250 mL Erlenmeyer flask containing 30 mL of 4% boric acid solution and drops of mixed indicator. The distillate was collected and then titrated with hydrochloric acid. A blank was made with the solvents only, and protein was calculated as nitrogen × 6.25 according to Association of Official Analytical Chemists (2005), following the Equation 1.

$$Protein(\%) = \frac{100\,x\,0.014\,x\,6.25\,x(Va - Vb)\,x\,f\,x\,N}{P} \quad (1)$$

Where V_a corresponds to the Volume of the sulphuric acid solution for titrating the material in ml; V_b is the volume of the sulphuric acid solution for titrating the blank in ml; N is the normality of the sulphuric acid solution; f = is the correction factor of the sulphuric acid solution, and P is the weight of the material in g.

Lipids

The method adapted from Bligh & Dyer (1959) was used to determine lipids. Initially, about 1g of the freeze-dried sample was weighed and then 6 mL of a mixture of chloroform: methanol (2:1 v/v) was added. The closed vials were homogenized for 1 hour. They were then centrifuged for 20 minutes at 3,000 rpm and the intermediate part containing the lipids was recovered using a pipette. The lipid fraction was dried with nitrogen and the lipid content determined by gravimetry.

Ashes

For the determination of ashes, about 3 g of *Scenedesmus* sp. was incinerated in an oven at 550 °C for 6 hours and then the remaining samples were weighed (Association of Official Agricultural Chemists, 2016).

Fiber

Crude fiber analysis was performed with the microalgae biomass moistened with acid digestion in a 1.25% sulfuric acid solution for 30 minutes, followed by alkaline digestion with 1.25% sodium hydroxide for another 30 minutes, with subsequent vacuum filtration and washing of the crucible with acetone and ethyl alcohol. The crucible was dried in an oven for 1 hour and then in a muffle furnace for 3 hours (Association of Official Agricultural Chemists, 2016). The crude fiber content was calculated by gravimetry.

Bioactive compounds

Phenolic compounds

The methodology proposed by Fonseca et al. (2020) was used to quantify total phenolic compounds. For the determination, an extract had to be prepared and for this, 1 g of the sample was added to a 15 mL centrifuge tube and 10 mL of methanol P.A. Homogenization was carried out in an ultraturrax (IKA, T18) at 10900 g for 1 min. Centrifugation was then carried out (Kasvi, K14-400) at 10900 g for 15 min at 15°C. The supernatant was collected and added to a centrifuge tube. 25 µL of the extract diluted in 190 µL of distilled water and 25 µL of Folin Ciocalteu Fenol 1N (Exodo Científica, Brazil) were used. The solution was homogenized and placed in a dark environment for 10 minutes. After this time, 50 µL of sodium carbonate (Synth, purity > 99%, Brazil) (1 M) was added and it was stored under the same conditions for 2 hours. The absorbance was read at 725 nm using a single-beam UV-Vis spectrophotometer (Bel, M51). A gallic acid curve with 6 concentration points was used to quantify the total phenolic compounds (y = 0.1887x + 0.1225, R^2 = 0.9648), where "y" is the absorbance and "x" is the equivalent gallic acid concentration.

Chlorophyll a, b, and total

To quantify the chlorophyll a, b and total contents, the methodology proposed by Lichtenthaler (1987) was followed, in which 1 g was weighed and 5 mL of 80% (v/v) acetone was added. The material was centrifuged at 2,000 rpm for 15 min and the supernatant transferred to a 25 mL volumetric flask, topping up with 80% (v/v) acetone. The absorbance of the extract was obtained by spectrophotometry at 647 and 663 nm using a UV-Vis spectrophotometer (Bel, M51).

Carotenoids

The methodology described by Rodriguez-Amaya (2001), with adaptations, was used to determine the carotenoid content. Around 5.0 g of the sample was homogenized in an Ultra Turrax (IKA T18) for 1 min at 11,000 rpm with 20 mL of ice-cold P.A. acetone. The mixture was filtered in a separating funnel, followed by the addition of 60 mL of acetone. 30 mL of hexane and 30 mL of distilled water were added to the funnel. After separating the phases, the polar phase was discarded and the apolar phase was washed with 3 aliquots of 30 mL of distilled water and placed in a 50 mL volumetric flask with hexane. Total carotenoids were determined using a spectrophotometer (Bel, M51) at 450 nm and calculated according to Equation 2.

$$Carotenoids\ (\mu g\,\beta - carotene / g) = \frac{\left(Abs\,x\,Solution\,volume\,x\,10^6\right)}{2500\,x\,100\,x\,Sample\,weight} \quad (2)$$

Where: A = absorbance of the solution at a wavelength of 450 nm for ß-carotene; V = final volume of the solution; = extinction coefficient or molar absorptivity coefficient of a pigment in a specific solvent (2500 for ß-carotene).

Simulation of the in vitro release of phenolic compounds in hydrophilic and hydrophobic medium

The release of phenolic compounds from the hydrogel with microalgae into the food simulator medium was carried out

according to Fonseca et al. (2020). 10 mg of the hydrogels (control and with microalgae) and of the microalgae (10 mg) were added to tubes with 1.5 ml of distilled water, and 1.5 mL of the hydrophilic medium simulator (10%, v/v ethanol), at room temperature (24 ± 3 °C) with gentle manual stirring. The same procedure was carried out with the hydrophobic medium (ethanol 50%, v/v) at room temperature (24 ± 3 °C) with manual stirring. At intervals of time (30, 60, 180, 240, 360 minutes) the concentration of phenolic compounds in the release medium was evaluated by the absorbance of the supernatant at a wavelength of 760 nm using a UV-Visible spectrophotometer (Bel Photonics) to evaluate the content of phenolic compounds using the Folin-Ciocalteu method adapted from Singleton et al. (1999). The samples were analyzed in triplicate, and the release profile in the hydrophilic and hydrophobic medium was presented as a percentage (%) and calculated according to Equation 3.

$$Release(\%) = \frac{\begin{matrix}Amount\ of\ phenolic\ compound \\ released\ into\ the\ simulating\ medium\end{matrix}}{\begin{matrix}Amount\ of\ microalgae\ phenolic \\ compound\ added\ to\ the\ hydrogel\end{matrix}} x100 \quad (3)$$

Fatty acid profile

The oil extracted from the microalgae by Bligh and Dyer was derivatized with BF_3. 250 mg of the oil was mixed with hexane and 6 mL of 2% (w/v) methanolic sodium hydroxide solution. The mixture was kept in a reflux system for 5 minutes. Afterwards, 5 mL of the BF_3/MeOH derivatizer was added and the reflux was maintained for 5 minutes. The solution was then transferred to a separating funnel and 20 mL of hexane was added until the phases were completely separated. The lower (aqueous) phase was then discarded and the upper part was filtered with sodium sulphate. The solution was rotary evaporated and finally washed with 1 mL of HPLC grade hexane and transferred to a vial for analysis by Gas Chromatography coupled to Mass Spectrometry.

To obtain the composition of the fatty acids present in the oil, a gas chromatograph (Shimadzu, model GC-2010) coupled to a mass spectrometer detector (GCMS-QP2020) was used, equipped with a SP 2560 fused silica capillary column (100 m x 0.25 mm x 0.10 µm). The volume of sample injected was 8 µL at a ratio of 1:50, in split mode. The interface and ion source temperature conditions were 280 °C and 200 °C, respectively. For the injector, a temperature of 200 °C was set using Helium carrier gas at a flow rate of 3 mL/min. For the column, the initial temperature was 100 °C and it remained at this temperature for 5 min. Subsequently, the temperature was raised to 250 °C at a constant heating rate of 5 °C/min.

Determination of metals

For acid decomposition, the method of Oreste et al. (2013) adapted by Antunes et al. (2021) was followed, which consists of weighing approximately 250 mg of sample directly into borosilicate tubes. Subsequently, 5.0 mL of HNO_3 was added, coupled to the reflux system and placed in the digester block at 150 °C for 2 hours. After this period, 1.0 mL of H_2O_2 was added and the solution returned to the block for another 30 min at 150 °C. At the end, the samples were removed from the block, allowed to cool, transferred to polypropylene flasks and equilibrated to 20 mL with distilled water.

A flame atomic absorption spectrometer (F AAS) was used to quantify the elements Cr, Cu, Fe, K, Na, Ni and Zn, while for K and Na, a flame atomic emission spectrometer (F-AES) model AAnalyst 200 (Perkin Elmer, Singapore) was employed, equipped with a hollow cathode lamp for each analyte (Lumina, Perkin Elmer) and a deuterium arc lamp for background correction, except for Na and K which were determined in atomic emission mode. The standard solutions used in the instrumental calibration were obtained from their respective stock solutions (1000 mg L^{-1} for: Cr, Cu, Fe, K, Na, Ni, and Zn) prepared in 1% (v/v) HNO_3 (Synth, Diadema, São Paulo, Brazil).

Formulation of microalgae extract and hydrogel

The microalgae extract was prepared by diluting 10 g of the microalgae biomass in 100 mL of distilled water, and kept in an ultrasound probe (Sonics Vibra-Cell VCX 500 - VCX 750) for 30 minutes at an amplitude of 35 microns. The commercial xanthan gum and sodium alginate hydrogel was prepared using the method of Ma et al. (2024) with modifications. A total of 1.5 g of xanthan gum powder and sodium alginate in a ratio of 1:1 (w/w) was mixed and poured into 100 mL of distilled water at 90 °C in a water bath, stirring at a speed of 200 rpm for 1 hour. After this, a transparent hydrogel was obtained without the addition of microalgae (control). After preparing the control hydrogel, another hydrogel was prepared using the same procedure, and after 1 hour of stirring at 90ºC, the *Scenesdesmus* sp. microalgae extract was added at a concentration of 10% (w/v). Finally, the solutions were placed in polyethylene Petri dishes and stored in a refrigerator (4 °C) for 24 hours for analysis. The methodology of the formulation of the hydrogels can be seen in Figure 2.

Fourier-transform infrared (FTIR) spectroscopy

FTIR analysis was conducted to identify the functional groups in the materials. A Shimadzu SPIRIT infrared spectrometer equipped with Attenuated Total Reflectance (ATR) was used for this purpose. The measurements were taken over a spectral range of 400 to 4000 cm^{-1}, with a resolution of 4 cm^{-1}, and a total of 45 scans were performed.

Citotoxicity assays

Cell culture

The mouse fibroblast strain (L929) was obtained from the American Type Culture Collection (ATCC, Rockville, MD, USA). The cells were maintained in Dulbecco's modified Eagle's medium (DMEM) containing $NaHCO_3$, HEPES, penicillin/streptomycin (100 U/L), fungizone (0.1%) and supplemented with 10% fetal bovine serum (FBS), with pH adjusted to 7.4. The cells were maintained at 5% CO_2 at 37°C under a humidified atmosphere until they reached 90% confluence.

Figure 2. Hydrogels graphical formulation and obtention.

After this, the strain was seeded in 96-well plates (density of 5 x 10^3 cells/well) for cytotoxicity and reactive oxygen species (ROS) assays (Pedra et al., 2022).

Treatment of the L929 strain

For each treatment (control hydrogel, microalgae extract, hydrogel with 1 g of microalgae, hydrogel with 2 g of microalgae), a stock solution was prepared at a concentration of 100 mg/mL (100 mg of the treatment in 1 mL of water for injections). The stock solution was diluted in DMEM with 10% SFB to obtain concentrations of 25, 50, 100, 200, 300, 400 and 500 µg/mL. Subsequently, the L929 strain was exposed to the different treatments for 24 and 48 hours, and cells exposed only to DMEM medium with 10% SFB were considered the control (Bona et al., 2024).

Cell viability and cell proliferation

The MTT (3-[4,5-dimethyl-thiazol-2-yl]-2-5-diphenyltetrazolium bromide) test is a colorimetric method used to assess cell viability, based on the ability of viable cells to reduce MTT. This process results in the formation of formazan crystals, which have a violet color and can be quantified by spectrophotometry (Mosmann, 1983). After the treatment periods, the DMEM medium was removed from the cells and the wells were washed with a balanced salt buffer free of calcium and magnesium salts (CMF). An MTT solution (0.5 mg/mL) was then added, and the cells were incubated for 90 min at 37 °C with 5% CO_2. After this, the solution was removed and the formazan precipitate dissolved in 50 µL of dimethylsulfoxide (DMSO). The absorbances were measured on a microplate reader (SpectraMax 190, Molecular Devices, San Jose, CA, USA) at wavelengths of 492 nm. The results were expressed as percentages of the control value.

In addition, the Sulforhodamine B (SRB) assay was carried out, which is a colorimetric method used to quantify cell proliferation. This test is based on the ability of the SRB dye to bind to basic amino acid residues under slightly acidic conditions (Pauwels et al., 2003). After the treatment period, the DMEM medium was removed and 50 µL of 50% trichloroacetic acid (TCA) was added to the wells for cell fixation. The cells were incubated for 45 min at 4 °C, followed by a wash with distilled water to remove the TCA. Next, 50 µL of SRB solution (0.4%) were added, and the cells incubated for 30 min at room temperature (protected from light). After incubation, the SRB solution was removed and the wells washed with 1% acetic acid until the unincorporated dye was completely removed. The residual dye was solubilized with 50 µL of a Tris solution (10 mM), and the absorbances were read on a microplate reader (SpectraMax 190) at a wavelength of 530 nm. The results were expressed as a percentage in relation to the control.

Reactive oxygen species

Reactive oxygen species (ROS) production was measured by the oxidation of 2',7'-dichlorodihydrofluorescein diacetate (DCFH-DA) into dichlorofluorescein (DCF) (Ali et al., 1992). After 48 hours of treatment, the cells were incubated with DCFH-DA for 30 minutes. Fluorescence was measured using a microplate reader (SpectraMax 190) at wavelengths of 488 and 525 nm, and ROS levels were expressed as a percentage relative to the control.

Statistical analysis

Statistical analysis was performed using GraphPad Prism 9.5.0 software. For the cytotoxicity data analysis, a one-way analysis of variance (ANOVA) was conducted, followed by Tukey's post-hoc test. Results were expressed as means ± standard error, with a significance level of $p<0.05$.

Results

Chemical analysis

The characterization of *Scenedesmus* sp. biomass is detailed in Table 1. The microalgae exhibited a high concentration of proteins, followed by lipids, fibers and ashes.

Content of bioactive compounds

The bioactive compound content values of *Scenedesmus* sp. biomass are presented in Table 2. Chlorophyll contents were measured in *Scenedesmus* sp. biomass, with values for chlorophyll a (0.98 ± 0.10 mg/kg), chlorophyll b (1.00 ± 0.20 mg/kg), and total chlorophyll (2.12 ± 0.2 mg/kg). Additionally, it was obtained 0.10 ± 0.10 (mg GAE/g) of phenolic compounds and 2.78 ± 0.20 (mg ß-carotene/g) of carotenoids.

Table 1. Physicochemical composition of the microalgae *Scenedesmus* sp.

Composition*	*Scenedesmus* sp. (%)
Moisture	76.88 ± 0.17
Protein	15.31 ± 0.20
Lipid	14.44 ± 0.74
Fiber	4.47 ± 0.10
Ash	3.11 ± 0.18

Mean (n=3) ± standard deviation. *Protein, lipid, fiber and ash - results expressed on a dry basis. Carbohydrates calculated by difference.

Table 2. Bioactive compounds in the microalgae *Scenedesmus* sp.

Bioactive compounds	*Scenedesmus* sp.
Phenolic compounds	0.10 ± 0.10 (mg GAE/g)
Chlorophyll a	0.98 ± 0.10 (mg/kg)
Chlorophyll b	1.00 ± 0.20 (mg/kg)
Total chlorophyll	2.12 ± 0.20 (mg/kg)
Carotenoids	2.78 ± 0.20 (mg ß-carotene/g)

GAE = gallic acid equivalent. Mean (n=3) ± standard deviation.

Fatty acid profile

The chromatographic analysis of fatty acids present in the oil of the microalgae *Scenedesmus* sp. is shown in Figure 3 and Table 3. As observed, palmitic acid was the predominant fatty acid found, reaching 41.95 ± 1.45%, followed by elaidic acid at 33.25 ± 1.42%. The microalgae *Scenedesmus* sp. was composed of 4 saturated fatty acids (myristic, pentadecanoic, palmitic, and stearic acids), 3 monounsaturated fatty acids (palmitoleic, oleic, and elaidic acids), and 1 polyunsaturated fatty acid (linolenic acid). Analyzing the fatty acid classes, saturated fatty acids were predominant, occupying an area of 49.30%. Regarding unsaturated fatty acids, an area of 40.72% was obtained. Additionally, there was a percentage of 8.19% of polyunsaturated fatty acids. The peaks that were not integrated had no correspondence in the equipment's library and were identified in Table 3 as others.

Determination of metals

Table 4 shows the concentrations obtained in the *Scenedesmus* sp. microalgae sample using the Flame Atomic Absorption Spectrometry technique. The ability of *Scenedesmus* sp. to absorb and accumulate metals, both essential and toxic, is one of its most notable characteristics, which makes it extremely useful in various biotechnological and environmental applications. In particular, the results found show that, among the essential metals, the highest concentrations were of K, Na, Fe, Cu, and Zn, which play important roles in biochemical and physiological processes, not only in the microalgae, but also in organisms that can benefit from this mineral-rich biomass.

Table 3. Fatty acid profile in microalgae oil.

Nº	Fatty acids	RT (min)	Relative Area (%)
1	Myristic acid (C14:0)	20.40	1.28 ± 0.18
2	Pentadecanoic acid (C15:0)	22.38	1.70 ± 0.03
3	Palmitoleic acid (C16:1)	26.15	5.05 ± 0.19
4	Palmitic acid (C16:0)	26.85	41.95 ± 1.45
5	Oleic acid (C18:1)	29.50	2.42 ± 0.19
6	Linolenic acid (C18:3)	31.95	8.19 ± 1.75
7	Elaidic acid (C18:1 trans)	32.18	33.25 ± 1.42
8	Stearic acid (C18:0)	33.00	4.37 ± 0.32
Others			1.79
∑FA saturated			49.30
∑FA unsaturated			40.72
∑FA polyunsaturated			8.19
Total			100

∑SFA = sum of fatty acids. RT = Retention time.

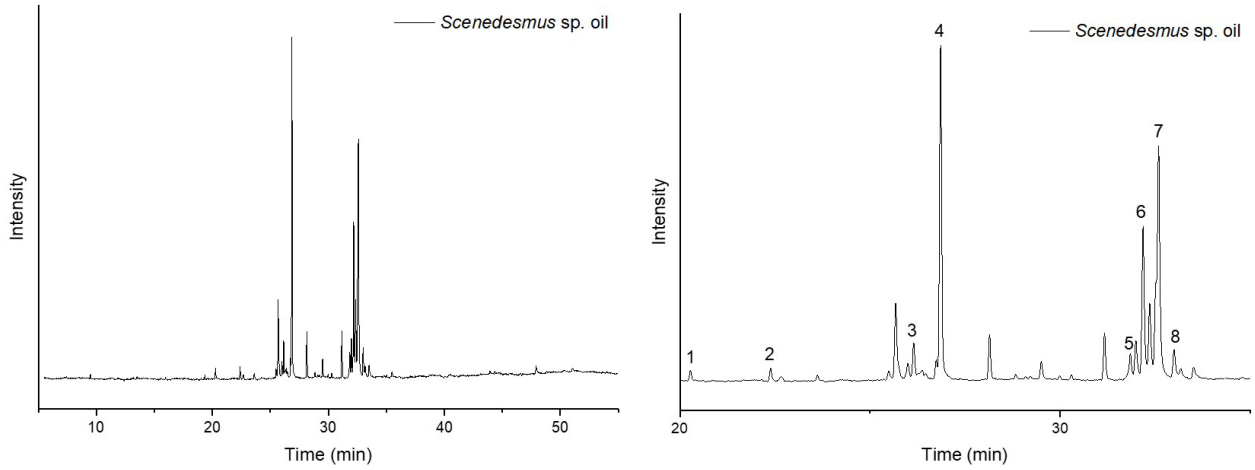

Figure 3. Chromatogram of the acid profile of *Scenedesmus* sp. oil.

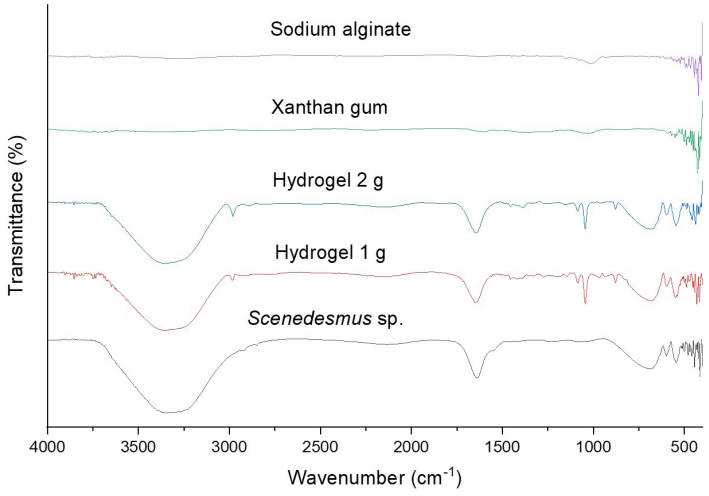

Figure 4. IR spectrum for xanthan gum, sodium alginate, *Scenedesmus* sp. and hydrogels.

On the other hand, metals with toxicity potential, such as Cr and Ni, showed lower concentrations, ranging from 2 to 4 mg.kg^{-1}. This reinforces the potential of *Scenedesmus* as an excellent candidate for bioremediation processes, since the microalgae can bioaccumulate toxic metals at manageable levels, while maintaining high levels of essential metals (Chew et al., 2017).

Fourier-transform infrared (FTIR) spectroscopy

Figure 4 shows the FTIR spectra of the xanthan gum, sodium alginate and hydrogels. The spectrum of xanthan gum exhbited bands at 3600-2980 cm^{-1}, 1600 cm^{-1} and 1407cm^{-1}. For the sodium alginate, bands were observed at 3694-2993 cm^{-1}, 2904 cm^{-1}, 1718 cm^{-1}, 1654 cm^{-1}, 1374–1450 cm^{-1}, 1025–1004 cm^{-1} and 950 to 750 cm^{-1}. In addition, the spectrum of microalgae *Scenedemus* sp., exhibited bands at 3300 cm^{-1}, 2923 cm^{-1} and 1640 cm^{-1}. Lastly, the hydrogels spectra exhibited characteristic bands related to the microalgae *Scenedemus* sp.

Table 4. Concentrations of elements present in the microalgae *Scenedesmus* sp.

Elements	*Scenedesmus* sp. (mg.kg^{-1}, n=3)
Cr	4.04 ± 0.28
Cu	6.65 ± 0.52
Fe	178.00 ± 13.00
K	455.00 ± 23.00
Na	537.00 ± 34.00
Ni	2.08 ± 0.21
Zn	4.34 ± 0.13

Values expressed as mean ± standard deviation.

Release of phenolic compounds from microalgae in hydrophilic and hydrophobic medium

The simulated release of phenolic compounds in 10% ethanol and 50% ethanol medium from the hydrogels and *Scenedesmus* sp. microalgae was evaluated (Figures 5 and 6). For the 50% ethanol medium, which simulates a hydrophobic system, 35.12% of phenolic compounds were released from the hydrogel with 1% microalgae, 29.25% for the (pure) microalgae, and 18.92% for the hydrogel with 2% microalgae (Figure 5). In general, there was a significant difference in the release of phenolic compounds when comparing the medium with 50% ethanol (hydrophobic) and 10% ethanol (hydrophilic), shown in Figures 5 and 6, respectively.

Cytotoxicity assays

The results regarding the cytotoxic effect of the *Scenedesmus* sp. extract, as well as hydrogels containing 1% and 2% of the microalgae at concentrations of 25 to 500 µg/mL, are shown in Figures 7 and 8. It can be seen that there was no change in viability or cell proliferation after exposure of the L929 strain of healthy fibroblasts to the different treatments for 24 or 48 hours.

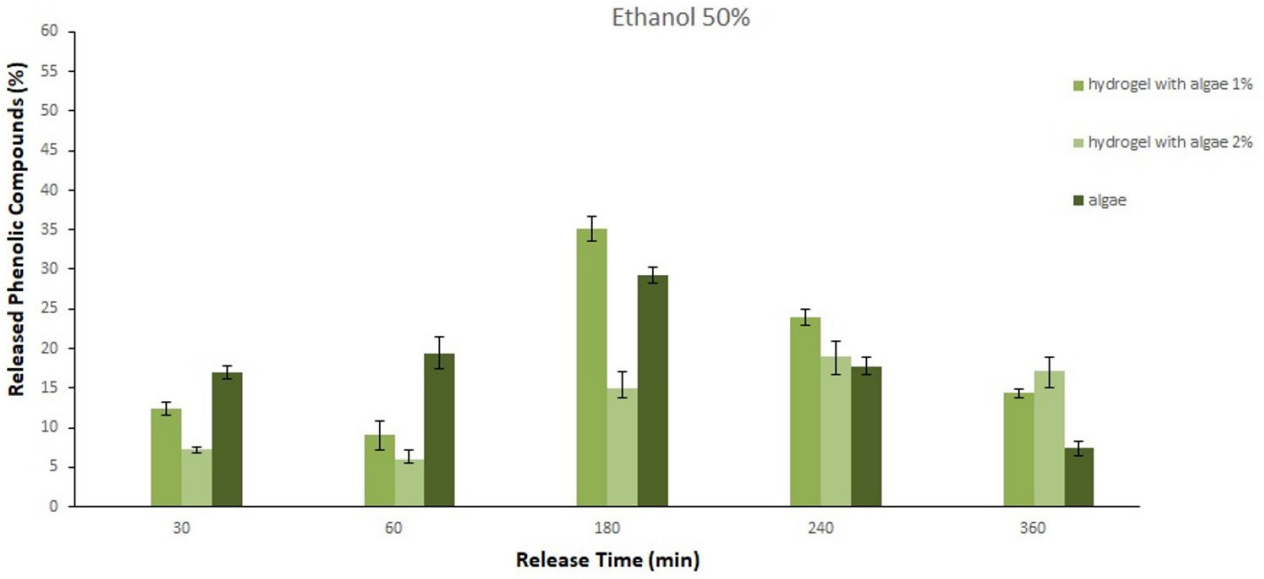

Figure 5. Phenolic compounds released after simulation in a hydrophobic medium of the digestion of *Scenedesmus* sp. microalgae and sodium alginate, xanthan gum and microalgae hydrogels (at 1 and 2%, w/w).

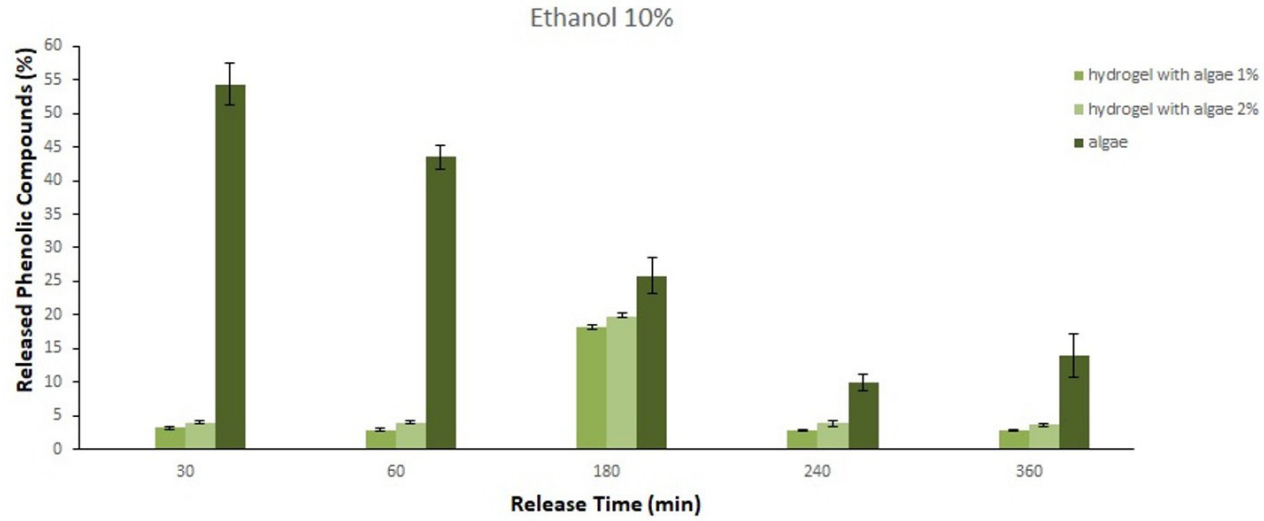

Figure 6. Phenolic compounds released after simulating the digestion of *Scenedesmus* sp. microalgae and sodium alginate, xanthan gum and microalgae hydrogels (1 and 2%, w/w) in a hydrophilic medium.

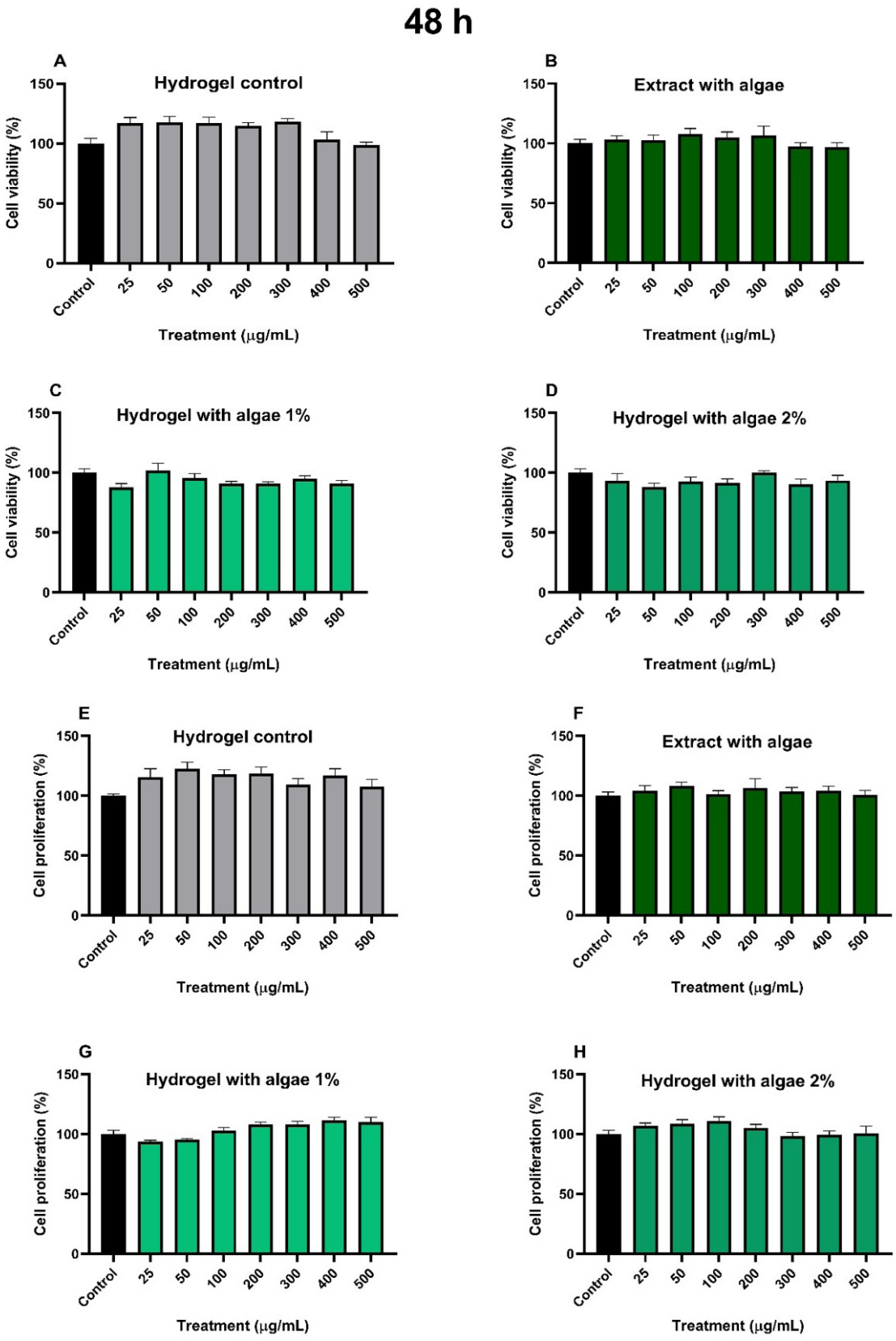

Figure 7. Effect of control hydrogel (A), microalgae extract (B), 1% microalgae hydrogel (C), 2% microalgae hydrogel (D), control hydrogel (E), microalgae extract (F), 1% microalgae hydrogel (G), 2% microalgae hydrogel (H) on the viability (A-D) and cell proliferation (E-H) of mouse fibroblast cells (L929) for 48 hours. Data were analyzed by one-way ANOVA followed by Tukey's test and expressed as mean ± standard error (n = 7-8).

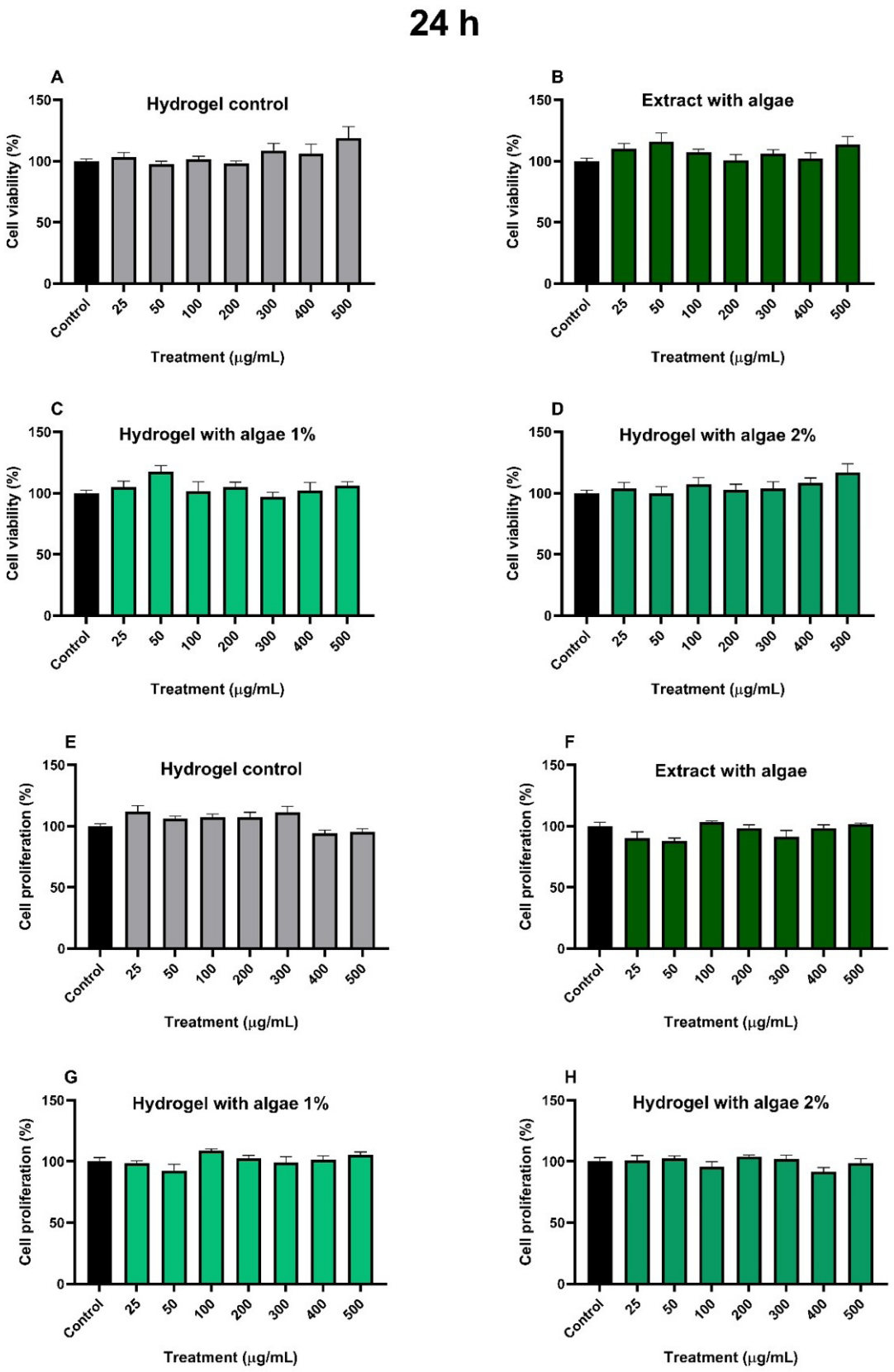

Figure 8. Effect of the control hydrogel (A), microalgae extract (B), 1% microalgae hydrogel (C), 2% microalgae hydrogel (D), control hydrogel (without microalgae) (E), microalgae extract (F), 1% microalgae hydrogel (G), 2% microalgae hydrogel (H) on the viability (A-D) and cell proliferation (E-H) of mouse fibroblast cells (L929) for 24 hours. Data were analyzed by one-way ANOVA followed by Tukey's test and expressed as mean ± standard error (n = 7-8).

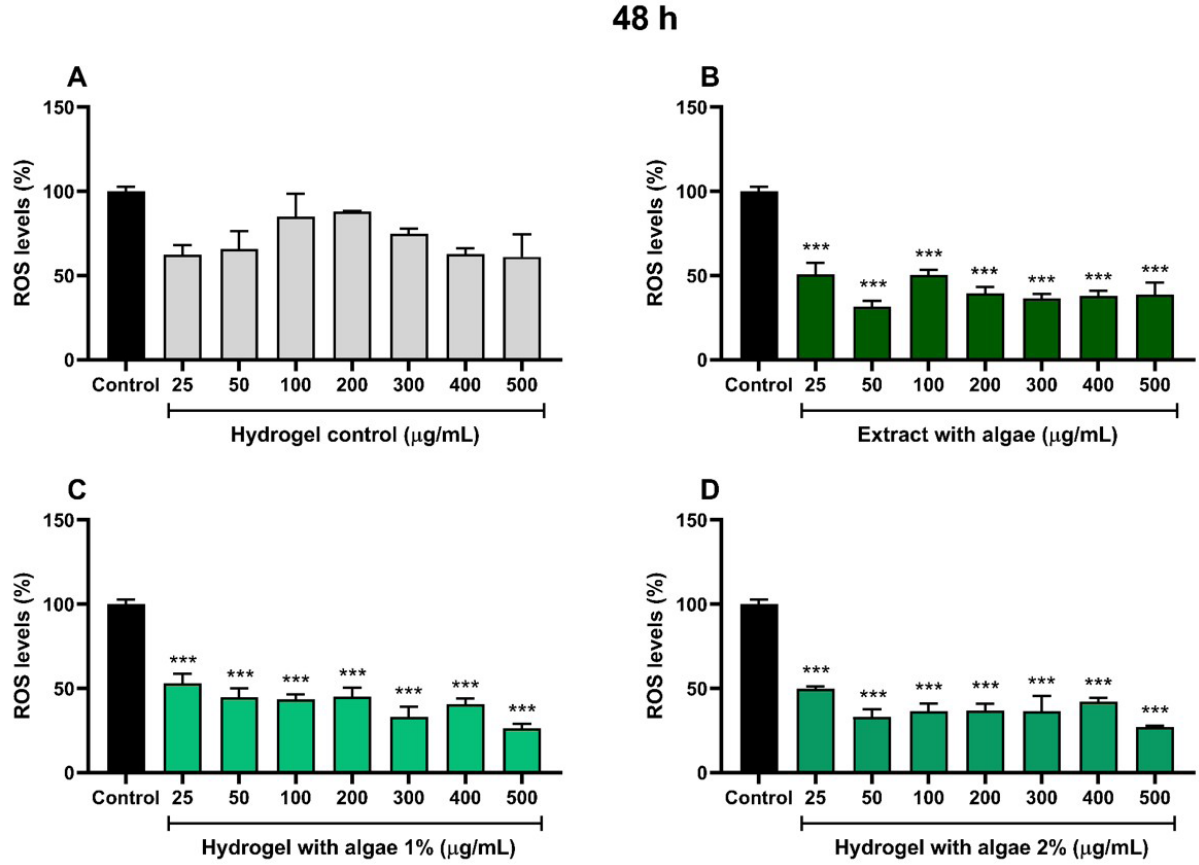

Figure 9. Levels of reactive oxygen species (ROS) in mouse fibroblast cell lines (L929) after 48 h of treatment. Treatment with control hydrogel (A), microalgae extract (B), 1% microalgae hydrogel (C) and 2% microalgae hydrogel (D). The results were expressed as a percentage of the control (ROS control value: 85.44 μmol DCF/mg protein). Data were analyzed by one-way ANOVA followed by Tukey's test and expressed as mean ± standard error (n=3). ***p<0.001 significantly different from the control group.

Furthermore, the control hydrogel also presented no cytotoxic effects at the concentrations and times evaluated.

Reactive oxygen species

Figure 9 shows the results for the effect of the control hydrogel, the *Scenedesmus* sp. extract and hydrogels containing 1% and 2% microalgae on ROS in the L929 strain after 48 h of treatment. The control hydrogel showed no significant changes in ROS levels (Figure 9A). On the other hand, treatment with the microalgae extract significantly reduced ROS levels at concentrations of 25, 50, 100, 200, 300, 400, and 500 μg/mL by 49.48, 68.58, 49.68, 60.51, 63.70, 62.22, and 61.13%, respectively, when compared to the control ($p<0.001$, Figure 9B).

It can also be seen that the 1% microalgae hydrogel significantly reduced ROS levels at all concentrations (25 to 500 μg/mL) by 47.11, 55.15, 56.62, 54.87, 66.86, 59.41, and 73.68%, respectively, when compared to the control ($p<0.001$, Figure 9C). In addition, the 2% microalgae hydrogel treatment significantly reduced ROS levels at concentrations of 25 to 500 μg/mL by 50.13, 66.82, 63.46, 63.07, 63.54, 57.99, and 73.01%, respectively, when compared to the control ($P<0.001$, Figure 9D).

Discussion

Chemical analysis

Souza et al. (2020) reported a lipid content of 16.72% using hexane extraction and ultrasound on freeze-dried *Scenedesmus* sp. biomass, along with a protein content of 53.77%. Similarly, Zhang et al. (2018) obtained 13.8% lipids using an enzyme-assisted method (cellulase, xylanase, and pectinase). Faruque et al. (2023) reported maximum lipid values of 29 and 32% using enrichment with 2 and 6% CO_2 mixed in the air during cultivation, respectively. Microalgae generally have low fiber content. The crude fiber values represent the fraction determined in acid digestion followed by basic digestion, without the use of enzymes, determining only the insoluble or partially soluble fibers (Uribe et al., 2019). Regarding ash content, Olsen et al. (2021) analyzed dry biomass of *Scenedesmus* sp. cultivated outdoors, obtaining 6.0% ash, 10.8% lipids, and 59.5% proteins. Amorim et al. (2020), using an open raceway system and an optimized protocol, reported an ash content of 36.2%, 5.5% lipids, and 33.9% proteins for dry *Scenedesmus* sp. biomass. These data highlight that cultivation conditions and biomass processing

significantly impact the final biochemical composition, which can be adjusted to obtain biomass with specific properties according to its intended application.

Content of bioactive compounds

The extraction of polyphenols is mainly influenced by the nature and polarity of the solvent (Moussa et al., 2021). Another study evaluated the total phenolic and carotenoid content of *Scenedesmus* sp. biomass, obtaining 5.40 mg GAE/g of phenolic compounds and 0.80 mg/g of carotenoids, extracted with ethanol/water and ethyl acetate, respectively (Bulut et al., 2019). Regarding total phenolic compounds, the study by Moussa et al. (2021) aimed to optimize the extraction of phenolic compounds from dry *Scenedesmus* sp. biomass cultivated in photobioreactors. The optimization process resulted in a maximum value of 28.11 mg/g of phenolic compounds using methanol and ultrasound at 4°C. The higher presence of phenolic compounds in polar solvents compared to solvents with lower polarity is well-documented in the literature (Bulut et al., 2019; Goiris et al., 2012), which can be attributed to the predominantly polar nature of these compounds. In this context, the quantity of phenolic compounds extracted in the present study can be explained by the lower polarity of methanol compared to the ethanol/water mixture, as well as various factors involved in the production stage of *Scenedesmus* sp. biomass, such as culture medium, pH, temperature, light intensity, and harvest time (León-Vaz et al., 2023; Bulut et al., 2019; Aremu et al., 2016).

Bioactive compounds such as phenolic compounds are commonly found in green and red seaweeds. The production and diversity of phenolic compounds in seaweeds vary among different taxonomic groups and species, being influenced when the algae undergo stress, leading to an increase in phenol production (Sadeghi et al., 2024). León-Vaz et al. (2023) observed that the levels of phenolic compounds and carotenoids in *Scenedesmus* sp. significantly increased under stress conditions. Shetty & Sibi (2015) reported that cultivation conditions (autotrophic, heterotrophic, and mixotrophic) significantly influenced the antioxidant capacity and phenolic content in strains of *S. obliquus*. In the study by Bulut et al. (2019), the lowest phenolic content recorded in the mixotrophic biomass of *Scenedesmus* sp. was 1.13 mg GAE.g^{-1}, while in the present study, the highest observed value was 0.10 GAE.g^{-1}. Aremu et al. (2016) highlighted that harvest time, nitrogen levels, and the choice of microalgae have a significant impact on phenolic content. These data demonstrate that the phenolic compound content in the biomass of *Scenedesmus* sp. is highly dependent on experimental conditions, especially regarding the choice of solvent and cultivation variables, allowing for the manipulation of these parameters to obtain higher levels of these compounds.

According to Ibrahim et al. (2021), carotenoids from the microalgae *Scenedesmus obliquus* (*S. obliquus*) cultivated under normal and stress conditions were extracted and quantified. The results indicated that stress conditions increased carotenoids from 0.63 mg.L^{-1} to 1.5 mg.L^{-1}. Six carotenoids were identified in *S. obliquus*, with a predominance of echinenone, diatoxanthin, and anthraxanthin. The carotenoid fraction extracted from *S. obliquus* demonstrated significant cytotoxic activity against hepatocellular carcinoma (HepG2), breast cancer (MCF-7), and colorectal cancer (HCT116) cells. The chlorophyll a, b, and total contents in the biomass of *Scenedesmus* sp. reflect this microalgae's ability to synthesize photosynthetic pigments under the cultivation conditions used. The values obtained for chlorophyll a (0.98 ± 0.10 mg/kg), chlorophyll b (1.00 ± 0.20 mg.kg^{-1}), and total chlorophyll (2.12 ± 0.2 mg.kg^{-1}) are consistent with previous studies that analyzed the biomass of *Scenedesmus* sp. under different cultivation conditions. According to Singh et al. (2022), chlorophyll concentrations in *Scenedesmus* species can vary significantly depending on nutrient availability, particularly nitrogen and phosphorus, as well as light intensity during cultivation.

In the present study, the observed levels of chlorophyll-a and chlorophyll-b were lower than those reported by Singh et al. (2022). In that study, the microalgae *Scenedesmus* sp. BHU1 was evaluated for the influence of sodium bicarbonate addition in the culture medium on the concentration of photosynthetic pigments. The results indicated that sodium bicarbonate supplementation significantly increased the levels of chlorophyll-a and chlorophyll-b. The highest chlorophyll-a content (8.32 µg mL^{-1}) was achieved in a culture supplemented with 12 mM of bicarbonate, representing an approximately 1.5-fold increase compared to the control culture. Additionally, bicarbonate addition raised the total chlorophyll content (a + b) to 11.51 µg mL^{-1}. However, a concentration of 20 mM bicarbonate resulted in a reduction in the chlorophyll-a/chlorophyll-b ratio and the carotenoid/total chlorophyll ratio compared to the control, which was attributed to an increase in pH, found to be unfavorable for microalgal growth. These results highlight that variations in pigment concentrations are influenced by environmental factors and the composition of the culture medium. The difference in behavior of pigments such as chlorophylls and carotenoids under different cultivation conditions for the same species emphasizes the importance of optimizing cultivation parameters to maximize the yield of biomolecules of interest.

Fatty acid profile

Our research group has considerable experience in the lipidomics of micro and macroalgae, as in the works of dos Santos et al. (2017), Pacheco et al. (2018), Santos et al. (2019), Do-Amaral et al. (2020), Berneira et al. (2020), de Freitas et al. (2020), de Santi et al. (2021) and Berneira et al. (2021). In this context, it was observed that the microalgae *Scenedesmus* sp. presents a balanced profile between saturated and unsaturated/polyunsaturated fatty acids (Table 3). Analyzing the fatty acid classes, saturated fatty acids were predominant, occupying an area of 49.30%, which is consistent with previous findings by Custódio et al. (2014), where a percentage of 54.9% of saturated fatty acids was reported. The three predominant saturated fatty acids found in membranes are myristic acid (14-C), palmitic acid (16-C), and stearic acid (18-C). High concentrations of saturated fatty acids (SFAs) and trans fatty acids are considered harmful, while high concentrations of unsaturated fatty acids are considered beneficial for cardiovascular health (Karacor & Cam, 2015). Myristic acid is found in low concentrations in human cell membranes and has antifungal, antiviral,

anticancer, antiparasitic, and immunomodulatory activities (Javid et al., 2021). Palmitic acid is the most common saturated fatty acid in the human body and is involved in crucial physiological functions, including maintaining the physical properties of cell membranes (Carta et al., 2017). Stearic acid is a saturated fatty acid that, unlike other saturated fatty acids, may have less negative impact on cardiovascular health. Studies suggest that it can be converted into oleic acid in the body, which may mitigate potential adverse effects (van Rooijen & Mensink, 2020). Meanwhile, the last saturated fatty acid found in the microalgae, pentadecanoic acid (C15:0), has an odd chain and is increasingly recognized as essential for supporting cardiometabolic and liver health (Dornan et al., 2021).

Regarding the unsaturated fatty acids found, oleic acid (OA) is the main component of olive oil (70-80%) and contributes to many of its health benefits (Lopez et al., 2014). It is obtained both through diet and synthesized in the body. OA is the most abundant monounsaturated fatty acid in the human diet, and in the body, it is the primary omega-9 monounsaturated fatty acid, produced by the action of stearoyl-CoA desaturase 1 (SCD1) from stearic acid through Δ9 desaturation (Santa-María et al., 2023). Elaidic acid is a trans fatty acid, and its serum levels tend to decrease with significant weight loss, as observed after bariatric surgery (Wrzosek et al., 2022). The monounsaturated fatty acid palmitoleic acid is one of the most abundant fatty acids in serum and tissues, particularly in adipose tissue and the liver (Frigolet & Gutiérrez-Aguilar, 2017). Regarding the only polyunsaturated fatty acid found, linolenic acid plays an essential role in cardiovascular health. Studies show that diets rich in polyunsaturated fatty acids, such as linolenic acid, can reduce serum saturated fatty acid content, contributing to better metabolic health (Naughton et al., 2016).

The saturated fatty acids present in the microalgae *Scenedesmus* sp. have a crucial role in the lipid composition and functional properties of this microalgae. Studies demonstrate that these fatty acids are important for the structure of cell membranes and can influence membrane fluidity, thereby affecting photosynthetic efficiency and adaptation to different environments (Los et al., 2013). Additionally, saturated fatty acids, such as palmitic acid, are often associated with nutritional and bioactive benefits, which increases interest in the use of *Scenedesmus* sp. for applications in nutrition and biofuels (Lucakova et al., 2022).

At the same time, the unsaturated fatty acids found in the microalgae *Scenedesmus* sp. are of great interest due to their nutritional benefits and potential industrial applications (Ishaq et al., 2016). The health benefits of consuming omega-3 polyunsaturated fatty acids are already well known, and their influence on brain development and the prevention of cardiovascular diseases has been proven in different epidemiological and clinical studies (Gheysen et al., 2018). In addition, recent studies highlight the potential of *Scenedesmus* sp. in the production of biofuels due to their favorable lipid composition, as well as their ability to grow in diverse environmental conditions (Makareviciene et al., 2011).

Determination of metals

Our research group has previously analyzed metals in macroalgae, as in the work of Picoloto et al. (2017). Thus, the biochemical components of microalgae, including mineral, carbohydrate and protein fractions, are highly versatile (Meng et al., 2022). These fractions can be used for a wide range of purposes, such as the production of chemicals, fuels, animal feed, biogas and value-added products such as nutraceuticals (Chew et al., 2017). The use of biomass for these purposes depends on both the mineral composition and the microalgae's ability to bioaccumulate metal ions, which adds value to its application in sustainable industrial processes (Meng et al., 2022; Mu et al., 2020).

The interaction between metals and hydrogels has received increasing attention, especially in the context of bioremediation and the controlled release of nutrients. Hydrogels, with their properties of high affinity for water, adjustable porosity and ease of handling, are promising materials for the capture and release of metal ions, such as Zn, Fe and Cu (Mu et al., 2020). The ability of hydrogels to gradually incorporate and release metals is especially valuable in extended nutrient release systems, such as in soil or aquatic environments (Mu et al., 2020). Furthermore, they can act by preventing, through complexation, the migration of metals with potential toxicity to plant roots (Zheng et al., 2023). The presence of high concentrations of Fe, for example, is an indication that *Scenedesmus* could be used in polluted environments, such as wastewater, where these metals are present in high quantities and need to be removed efficiently (Dias et al., 2019).

In addition, its ability to transport other compounds, such as drugs and nutraceuticals, broadens its applications, from the agricultural field, where it can promote plant growth by releasing micronutrients, to the medical field, where it can be used in regenerative therapies (Pereira et al., 2021; Quadrado et al., 2022). The combination of the bioaccumulation capacity of *Scenedesmus* and the versatility of hydrogels offers new opportunities in the production of hybrid materials for a wide range of applications. The use of polysaccharides, both natural and synthetic, in the manufacture of hydrogels provides the possibility of creating materials with properties capable of retaining and releasing the essential metals bioaccumulated by the microalgae in a controlled manner.

Fourier-transform infrared (FTIR) spectroscopy

In the infrared spectrum (Figure 4) it is possible to observe that the xanthan gum presented the bands at 3600-2980 cm^{-1}, which are relative to O-H stretching vibrations with intermolecular H bonding and C-H stretching, respectively. The medium intensity band relative to asymmetrical C-O stretching vibration at 1600 cm^{-1} and a symmetrical C=O stretching at 1407cm^{-1}, both from the carboxylate anion (COO^-) of the xanthan gum (Pawlicka et al., 2019). Meanwhile, in the spectra of sodium alginate, a broad band centred at 3694-2993 cm^{-1} is assigned to hydrogen bonded O–H stretching vibrations and a weak signal at 2904 cm^{-1} attributed to C–H stretching vibrations. A small-signal appears between 1718 cm^{-1}, corresponding to the carbonyl group as the carboxylic acid ester form (C=O). The abroad bands at 1654 cm^{-1} suggests an O-C-O carboxylate asymmetric stretching (Belattmania et al., 2020). The bands located at 1374–1450 cm^{-1} are assigned to C-OH deformation

vibration with the involvement of the symmetric stretching vibration of O-C-O (Papageorgiou et al., 2010). According to previous reports, the bands at 1025–1004 cm^{-1} can be attributed to the C-O group (Belattmania et al., 2020). The anomeric region (950 to 750 cm^{-1}) is the most discussed in carbohydrates (Leal et al., 2008). The FTIR spectra of *Scenedesmus* sp. revealed an absorbance peak at 3300 cm^{-1}, which corresponded to the N-H stretching vibration. The alcoholic O-H stretching vibration is attributed to the peak at 2923 cm^{-1} and the N-H binding vibration to the peak at 1640 cm^{-1} (Waqar et al., 2023). These same bands can be seen in the spectra of hydrogels with different concentrations of microalgae.

Release of phenolic compounds from microalgae in hydrophilic and hydrophobic medium

It can be seen in Figure 5 that the hydrogel allowed a slow and gradual release of the phenolic compounds in the hydrophobic medium over the release time analyzed. The release of phenolic compounds from the (pure) microalgae was rapid, with 16.97% of the phenols present in the microalgae being released after 30 minutes. After 360 min there was a decrease in the percentage of phenolics in the (pure) microalgae, with 7.36%, attributed to probable degradation. In a hydrophilic medium (10% ethanol), the phenolic compounds in the hydrogel released low quantities in the first 60 min. The highest percentage of phenolic compounds released was 19.73 and 18.11% for the hydrogels with 2 and 1% microalgae, respectively. However, for the (pure) microalgae there was a rapid release of phenolics, 54.33% after 30 min in the hydrophilic medium. The hydrogel possibly promoted greater solubilization of the microalgae's phenolic compounds in hydrophobic conditions, resulting in a higher percentage of release.

The results obtained show that the hydrogel served as a delivery vehicle for the microalgae's phenolic compounds, even after being simulated in different medium. The hydrogels protect the compounds from degradation in an environment with different conditions. In this context, it can be suggested that the hydrogels produced have the potential to be applied in the formulation of pharmaceutical products, foodstuffs and different biotechnological applications.

Cytotoxicity assays

The results of the cytotoxicity tests obtained are consistent with the study carried out by Cho et al. (2023), who reported that the extract of *Scenedesmus* deserticola JD052, extracted with different types of solvent, did not show significant cytotoxicity on the viability of healthy human dermal fibroblasts (nHDFs). In addition, Ma et al. (2024) showed that the hydrogel composed of soy protein and sodium alginate (SPI-SA) had no toxic effect on L929 cells, which favors cell growth in the pores of these materials, highlighting the potential of these hydrogels for applications in in vitro studies.

It should be noted that the L929 mouse fibroblast cell line is widely used to assess the biocompatibility of hydrogels (Ma et al., 2024). Studies have shown that hydrogels such as gelatin/dextran oxide (Guan et al., 2022) and hyaluronic acid/polylysine (Guo et al., 2021) offer a favorable microenvironment for cell growth. These hydrogels, when tested on L929 cells, showed good cell compatibility and adequate space for cultivation, indicating their potential in biomaterials and pharmacological research (Guo et al., 2021).

Reactive oxygen species

Considering that treatment with the control hydrogel did not induce significant changes in the ROS levels of the L929 strain, it is possible to infer that the reduction observed in the levels of this parameter after treatment with the hydrogels containing microalgae is not caused by the components of the hydrogel itself, but by the presence of the microalgae. It is also possible to observe that treatment with the hydrogels containing *Scenedesmus* sp. at the highest concentration used (500 µg/mL) promoted a greater reduction in ROS levels compared to the extract, inferring that the hydrogel may potentiate the effects of the microalgae.

It is important to notice that this observed effect may be largely due to the rich bioactive composition present in *Scenedesmus* sp. Among the existing microalgae species, *Scenedesmus obliquus* has a large number of carotenoids, more specifically ß-carotene and lutein, which perform a potent antioxidant capacity, since they act by neutralizing free radicals such as singlet oxygen and peroxyl (Nascimento et al., 2019, 2021). In addition, an in vivo study evaluated the effect of *S. obliquus* microalgae biomass at concentrations of 400 and 800 mg/kg on different tissues, showing a reduction in lipid peroxidation levels using the thiobarbituric acid reactive substances assay, corroborating with the results found in this study. These findings demonstrate the significant antioxidant activity of this microalga, highlighting its potential use for promoting human health (Nascimento et al., 2019).

Conclusions

This study highlighted the biotechnological potential of microalgae of the genus *Scenedesmus* in the formulation of bioactive hydrogels. The characterization of the microalgal biomass revealed the presence of valuable phenolic compounds, carotenoids, chlorophylls, and various fatty acids, which, under optimized cultivation conditions, can be significantly enriched. The addition of *Scenedesmus* sp. biomass into bioproducts not only brings these antioxidant compounds into the material but also offers additional nutritional advantages through the inclusion of essential fatty acids and high-quality proteins. These fatty acids, particularly omega-3 and omega-6, are known for their roles in anti-inflammatory processes, cellular health, and skin barrier function, adding further bioactivity to the hydrogels. Moreover, the phenolic compounds found in *Scenedesmus* sp. contribute to its antioxidant profile, supporting the neutralization of ROS and enhancing cell protection. Additionally, the proteins present in the microalgae biomass also offer potential therapeutic applications, as they include bioactive peptides with possible roles in skin health and tissue repair. By leveraging these compounds, hydrogels containing *Scenedesmus* sp. biomass

are promising multifunctional bioactive materials that can provide controlled release of antioxidants, fatty acids, and proteins over time. The production of these hydrogels enables the development of materials with characteristics suited for both retention and gradual release of bioactive compounds, allowing a sustained efficacy in different applications. Future studies should concentrate on optimizing cultivation practices, characterizing the bioactive potential of the proteins and fatty acids in new biological models, and investigating industrial applications for these compounds. This approach can significantly advance our knowledge and technologies involving microalgae, opening pathways for new biotechnological innovations.

Conflict of interests

The authors declare that they have no competing interests. Funding: This work was supported by FAPERGS (22/2551- 0000840-2), the Brazilian Coordination for the Improvement of Higher Education Personnel (CAPES, code 001) and the National Council for Scientific and Technological Development (CNPq).

Acknowledgements

The authors are thankful to the Research Support Foundation of the State of Rio Grande do Sul (BR) FAPERGS (22/2551-0000840-2) for the project “Supplements and products derived from alternative sources for animal welfare”, the Brazilian Coordination for the Improvement of Higher Education Personnel (CAPES, code 001) and the National Council for Scientific and Technological Development (CNPq).

References

Albuquerque, B. R., Heleno, S., Oliveira, M., Barros, L., & Ferreira, I. (2021). Phenolic compounds: Current industrial applications, limitations and future challenges. *Food & Function*, *12*(1), 14-29. http://doi.org/10.1039/D0FO02324H. PMid:33242057.

Ali, S., Lebel, C., & Bondy, S. (1992). Reactive oxygen species formation as a biomarker of methylmercury and trimethyltin neurotoxicity. *Neurotoxicol*, *13*(3), 637-648. PMid:1475065.

Al-Mossawi, M., Warren, H., Molino, P., Calvert, P., & in het Panhuis, M. (2021). Living electrodes based on green algae in hydrogels. *Materials Advances*, *2*(4), 1369-1377. http://doi.org/10.1039/D0MA00985G.

Amorim, M., Soares, J., Vieira, B., Batista-Silva, W., & Martins, M. (2020). Extração de proteínas da microalga *Scenedesmus obliquus* BR003 seguida de extração lipídica da biomassa úmida desproteinizada usando hexano e acetato de etila. *Bioresource Technology*, *307*, 123190. http://doi.org/10.1016/j.biortech.2020.123190. PMid:32213445.

Antunes, B. D. F., Otero, D. M., Bonemann, D. H., Ribeiro, A. S., Jacques, A. C., & Zambiazi, R. C. (2021). Evaluation of physicochemical, bioactive composition and profile of fatty acids in leaves of different olive cultivars. *Revista Ceres*, *68*(6), 511-520. http://doi.org/10.1590/0034-737x202168060002.

AOAC (2005) Official Methods of Analysis of Association of Official Analytical Chemists. 18th Edition, Washington, DC.

Aremu, A., Masondo, N., Molnár, Z., Stirk, W., Ördög, V., & Van Staden, J. (2016). Changes in phytochemical content and pharmacological activities of three *Chlorella* strains grown in different nitrogen conditions. *Journal of Applied Phycology*, *28*(1), 149-159. http://doi.org/10.1007/s10811-015-0568-7.

Association of Official Agricultural Chemists. (2016). *2016 Official methods of analysis* (20th ed.). AOAC International.

Belattmania, Z., Kaidi, S., El Atouani, S., Katif, C., Bentiss, F., Jama, C., Reani, A., Sabour, B., & Vasconcelos, V. (2020). Isolation and FTIR-ATR and 1H NMR characterization of alginates from the main alginophyte species of the atlantic coast of Morocco. *Molecules*, *25*(18), 4335. http://doi.org/10.3390/molecules25184335. PMid:32971782.

Berneira, L., Santi, I., Silva, C., Venzke, D., Colepicolo, P., Vaucher, R., Santos, M., & Pereira, C. (2021). Bioactivity and composition of lipophilic metabolites extracted from Antarctic macroalgae. *Brazilian Journal of Microbiology*, *52*(3), 1275-1285. http://doi.org/10.1007/s42770-021-00475-6. PMid:33835420.

Berneira, L., Silva, C., Poletti, T., Ritter, M., dos Santos, M., Colepicolo, P., & de Pereira, C. (2020). Evaluation of the volatile composition and fatty acid profile of seven Antarctic macroalgae. *Journal of Applied Phycology*, *32*(5), 3319-3329. http://doi.org/10.1007/s10811-020-02170-9.

Bligh, E. G., & Dyer, W. (1959). A rapid method of total lipid extraction and purification. *Canadian Journal of Biochemistry and Physiology*, *37*(8), 911-917. http://doi.org/10.1139/o59-099. PMid:13671378.

Bona, N., Pedra, N., Spohr, L., Santos, F., Saraiva, J., Carvalho, F., Fernandes, M., Fernandes, A., Saraiva, N., Martins, M., Tavares, R., Spanevello, R., Aguiar, M., & Stefanello, F. (2024). Antitumoral Activity of Cecropia Pachystachya Leaves Extract in Vitro and in Vivo Model of Rat Glioma: Brain and Blood Effects. *Molecular Neurobiology*, *61*(10), 8234-8252. http://doi.org/10.1007/s12035-024-04086-8. PMid:38483655.

Bulut, O., Akın, D., Sönmez, Ç., Öktem, A., Yücel, M., & Öktem, H. (2019). Phenolic compounds, carotenoids, and antioxidant capacities of a thermo-tolerant *Scenedesmus* sp.(Chlorophyta) extracted with different solvents. *Journal of Applied Phycology*, *31*(3), 1675-1683. http://doi.org/10.1007/s10811-018-1726-5.

Carta, G., Murru, E., Banni, S., & Manca, C. (2017). Palmitic acid: Physiological role, metabolism and nutritional implications. *Frontiers in Physiology*, *8*, 902. http://doi.org/10.3389/fphys.2017.00902. PMid:29167646.

Chen, H., Guo, Y., Zhang, Z., Mao, W., Shen, C., Xiong, W., Yao, Y., Zhao, X., Hu, Y., Zou, Z., & Wu, J. (2021). Symbiotic algae-bacteria dressing for producing hydrogen to accelerate diabetic wound healing. *Nano Letters*, *22*(1), 229-237. http://doi.org/10.1021/acs.nanolett.1c03693. PMid:34928162.

Chew, K., Yap, J., Show, P., Suan, N., Juan, J., Ling, T., Lee, D., & Chang, J. (2017). Microalgae biorefinery: High value products perspectives. *Bioresource Technology*, *229*, 53-62. http://doi.org/10.1016/j.biortech.2017.01.006. PMid:28107722.

Ching, S., Bansal, N., & Bhandari, B. (2017). Alginate gel particles-A review of production techniques and physical properties. *Critical Reviews in Food Science and Nutrition*, *57*(6), 1133-1152. http://doi.org/10.1080/10408398.2014.965773. PMid:25976619.

Cho, D., Yun, J., Heo, J., Lee, I., Lee, Y., Bae, S., Yun, B., & Kim, H. (2023). Identification of Loliolide with Anti-Aging Properties from *Scenedesmus deserticola* JD052. *Journal of Microbiology and Biotechnology*, *33*(9), 1250-1256. http://doi.org/10.4014/jmb.2304.04044. PMid:37317620.

Custódio, L., Soares, F., Pereira, H., Barreira, L., Vizetto-Duarte, C., Rodrigues, M. J., Rauter, A. P., Alberício, F., & Varela, J. (2014). Fatty acid composition and biological activities of *Isochrysis galbana* T-ISO, *Tetraselmis* sp. and *Scenedesmus* sp.: Possible application in the pharmaceutical and functional

food industries. *Journal of Applied Phycology*, *26*(1), 151-161. http://doi.org/10.1007/s10811-013-0098-0.

Dias, G., Hipólito, M., Santos, F., Lourega, R., Mattia, J., Eichler, P., & Alves, J. (2019). Biorremediação de efluentes por meio da aplicação de microalgas – uma revisão. *Quimica Nova*, *42*, 891-899. http://doi.org/10.21577/0100-4042.20170393.

Do-Amaral, C., Pacheco, B., Segatto, N., Paschoal, J., Santos, M., Seixas, F., Pereira, C., Astorga-España, M., Mansilla, A., & Collares, T. (2020). Lipidic profile of sub-Antarctic seaweed *Mazzaella laminarioides* (Gigartinales, Rhodophyta) in distinct developmental phases and cell cytotoxicity in bladder cancer. *Algal Research*, *48*, 101936. http://doi.org/10.1016/j.algal.2020.101936.

Dornan, K., Gunenc, A., Oomah, B., & Hosseinian, F. (2021). Odd chain fatty acids and odd chain phenolic lipids (alkylresorcinols) are essential for diet. *Journal of the American Oil Chemists' Society*, *98*(8), 813-824. http://doi.org/10.1002/aocs.12507.

Faruque, M., Hossain, M., & Razzak, S. (2023). Photoautotrophic cultivation, lipid enhancement, and dry biomass characterization of microalgae *scenedesmus* dimorphus for bioenergy application. *Arabian Journal for Science and Engineering*, *48*(12), 16263-16280. http://doi.org/10.1007/s13369-023-08187-9.

Fonseca, L. M., Oliveira, J. P., Crizel, R., Silva, F., Zavareze, E., & Borges, C. (2020). Electrospun Starch Fibers Loaded with Pinhão (Araucaria angustifolia) Coat Extract Rich in Phenolic Compounds. *Food Biophysics*, *15*(3), 355-367. http://doi.org/10.1007/s11483-020-09629-9.

Freitas, F., Alves, V., & Reis, M. (2015). Bacterial polysaccharides: production and applications in cosmetic industry. In K. Ramawat & JM. Mérillon (Eds.), *Polysaccharides* (pp. 2017-2043). Springer. http://doi.org/10.1007/978-3-319-16298-0_63.

Freitas, S., Berneira, L., dos Santos, M., Poletti, T., Mansilla, A., Astorga-España, M., Garcia, M., Hartwig, D., Hübner, S., & de Pereira, C. (2020). Bioactivity evaluation and composition of extracts from sub-Antarctic macroalgae *Mazzaella laminarioides* at distinct development phases. *Revista Brasileira de Botanica. Brazilian Journal of Botany*, *43*(4), 689-696. http://doi.org/10.1007/s40415-020-00661-0.

Frigolet, M., & Gutiérrez-Aguilar, R. (2017). The role of the novel lipokine palmitoleic acid in health and disease. *Advances in Nutrition*, *8*(1), 173S-181S. http://doi.org/10.3945/an.115.011130. PMid:28096141.

Furtado, I., Sydney, E., Rodrigues, S., & Sydney, A. (2022). Xanthan gum: Applications, challenges, and advantages of this asset of biotechnological origin. *Biotechnology Research and Innovation Journal*, *6*(1), e202204. http://doi.org/10.4322/biori.202205.

Gheysen, L., Bernaerts, T., Bruneel, C., Goiris, K., Van Durme, J., Van Loey, A., Cooman, L., & Foubert, I. (2018). Impact of processing on n-3 LC-PUFA in model systems enriched with microalgae. *Food Chemistry*, *268*, 441-450. http://doi.org/10.1016/j.foodchem.2018.06.112. PMid:30064781.

Goiris, K., Muylaert, K., Fraeye, I., Foubert, I., De Brabanter, J., & De Cooman, L. (2012). Antioxidant potential of microalgae in relation to their phenolic and carotenoid content. *Journal of Applied Phycology*, *24*(6), 1477-1486. http://doi.org/10.1007/s10811-012-9804-6.

Guan, S., Zhang, K., Cui, L., Liang, J., Li, J., & Guan, F. (2022). Injectable gelatin/oxidized dextran hydrogel loaded with apocynin for skin tissue regeneration. *Biomaterials advances*, *133*, 112604. http://doi.org/10.1016/j.msec.2021.112604. PMid:35527157.

Guillard, R., & Lorenzen, C. (1972). Yellow-Green Algae with Chlorophyllide C. *Journal of Phycology*, *8*(1), 10-14. http://doi.org/10.1111/j.1529-8817.1972.tb03995.x.

Guiry, M. D. (2014). Scenedesmus meyen, 1829. In M.D. Guiry, & G.M. Guiry, (Eds.), *AlgaeBase*. National University of Ireland. https://www.algaebase.org

Guo, Y., Bao, Y., Sun, K., Chang, C., & Liu, W. (2021). Effects of covalent interactions and gel characteristics on soy protein-tannic acid conjugates prepared under alkaline conditions. *Food Hydrocolloids*, *112*, 106293. http://doi.org/10.1016/j.foodhyd.2020.106293.

Ibrahim, N., Matloub, A., El-Sayed, A., Aly, H, AbdElsamiae, A. (2021). Phytochemical and biological studies of carotenoids in some microalgae (*Dunaliella salina, Scenedesmus* obliquus and *Spirulina platenses*). *Egyptian Journal of Chemistry*, *64*(5), 2343-2353. http://doi.org/10.21608/ejchem.2021.60663.3306.

Ishaq, A., Matias-Peralta, H., & Basr, H. (2016). Bioactive compounds from green microalga-*Scenedesmus* and its potential applications: a brief review. *Pertanika. Journal of Tropical Agricultural Science*, 39(1), 1-16.

Javed, F., Aslam, M., Rashid, N., Shamair, Z., Khan, A. L., Yasin, M., Fazal, T., Hafeez, A., Rehman, F., Rehman, M., Khan, Z., Iqbal, J., & Bazmi, A. (2019). Microalgae-based biofuels, resource recovery and wastewater treatment: A pathway towards sustainable biorefinery. *Fuel*, *255*, 115826. http://doi.org/10.1016/j.fuel.2019.115826.

Javid, S., Purohit, M., Kumar, H., Ramya, K., Mithuna, N., Salahuddin, M., & Kumar, B. (2021). Semisynthesis of myristic acid derivatives and their biological activities: A critical insight. *Journal of Biologically Active Products from Nature*, *10*(6), 455-472. http://doi.org/10.1080/22311866.2020.1865836.

Karacor, K., & Cam, M. (2015). Effects of oleic acid. *Medical Science and Discovery*, *2*(1), 125-132. http://doi.org/10.36472/msd.v2i1.53.

Kopač, T., Boček, Ž., van Midden, K. P., Klemenčič, M., & Ručigaj, A. (2023). Encapsulation of living photosynthetic organisms in alginate-gelatin hydrogels for controlled cell growth and oxygen production. *Biochemical Engineering Journal*, *199*, 109070. http://doi.org/10.1016/j.bej.2023.109070.

Leal, D., Matsuhiro, B., Rossi, M., & Caruso, F. (2008). FT-IR spectra of alginic acid block fractions in three species of brown seaweeds. *Carbohydrate Research*, *343*(2), 308-316. http://doi.org/10.1016/j.carres.2007.10.016. PMid:18048014.

León-Vaz, A., León, R., Vigara, J., & Funk, C. (2023). Exploring Nordic microalgae as a potential novel source of antioxidant and bioactive compounds. *New Biotechnology*, *73*, 1-8. http://doi.org/10.1016/j.nbt.2022.12.001. PMid:36513346.

Lichtenthaler, H. K. (1987). Chlorophylls and carotenoids: pigments of photosynthetic biomembranes. In: L. Packer & R. Douce (Eds.), *Plant cell membranes* (Methods in Enzymology Book Series, Vol. 148, pp. 350-382). Academic Press. http://doi.org/10.1016/0076-6879(87)48036-1.

Liu, Y., Ren, X., Fan, C., Wu, W., Zhang, W., & Wang, Y. (2022). Health benefits, food applications, and sustainability of Microalgae-Derived N-3 PUFA. *Foods*, *11*(13), 1883. http://doi.org/10.3390/foods11131883. PMid:35804698.

Lopez, S., Bermudez, B., Paz, S., Jaramillo, S., Varela, L., Ortega-Gomez, A., Abia, R., & Muriana, F. (2014). Membrane Composition and Dynamics: A Target of Bioactive Virgin Olive Oil Constituents. *Biochimica et Biophysica Acta*, *1838*(6), 1638-1656. http://doi.org/10.1016/j.bbamem.2014.01.007. PMid:24440426.

Los, D., Mironov, K., & Allakhverdiev, S. (2013). Regulatory role of membrane fluidity in gene expression and physiological functions. *Photosynthesis Research*, *116*(2-3), 489-509. http://doi.org/10.1007/s11120-013-9823-4. PMid:23605242.

Lucakova, S., Branyikova, I., & Hayes, M. (2022). Microalgal proteins and bioactives for food, feed, and other applications. *Applied Sciences (Basel, Switzerland)*, *12*(9), 4402. http://doi.org/10.3390/app12094402.

Ma, C., Gao, X., Yang, Y., Bian, X., Wang, B., Liu, X., Wang, Y., Su, D., Zhang, G., Qu, L., & Zhang, N. (2024). The three-dimensional culture of L929 and C2C12 cells based on SPI-SA interpenetrating network hydrogel scaffold with excellent mechanical properties. *Frontiers in Bioengineering and Biotechnology*, *11*, 1329183. http://doi.org/10.3389/fbioe.2023.1329183. PMid:38268933.

Makareviciene, V., Andrulevičiūtė, V., Skorupskaitė, V., & Kasperovičienė, J. (2011). Cultivation of microalgae *Chlorella* sp. and *Scenedesmus* sp. as a potentional biofuel

feedstock. *Environmental Research, Engineering and Management*, 57(3), 21-27.

Mendonça, H. V., Assemany, P., Abreu, M., Couto, E., Maciel, A. M., Duarte, R. L., Santos, M. G. B., & Reis, A. (2021). Microalgae in a global world: New solutions for old problems? *Renewable Energy*, *165*, 842-862. http://doi.org/10.1016/j.renene.2020.11.014.

Meng, W., Mu, T., & Marco, G. (2022). Seaweeds and microalgal biomass: The future of food and nutraceuticals. *Future Foods*, *10*, 183-201. http://doi.org/10.1016/B978-0-323-91001-9.00014-1.

Mobin, S., & Alam, F. (2017). Some promising microalgal species for commercial applications: A review. *Energy Procedia*, *110*, 510-517. http://doi.org/10.1016/j.egypro.2017.03.177.

Mosmann, T. (1983). Rapid colorimetric assay for cellular growth and survival: Application to proliferation and cytotoxicity assays. *Journal of Immunological Methods*, *65*(1-2), 55-63. http://doi.org/10.1016/0022-1759(83)90303-4. PMid:6606682.

Moussa, I., Masmoudi, M., Choura, S., Chamkha, M., & Sayadi, S. (2021). Extraction optimization using response surface methodology and evaluation of the antioxidant and antimicrobial potential of polyphenols in *Scenedesmus* sp. and *Chlorella* sp. *Biomass Conversion and Biorefinery*, *13*(8), 7185-7198. http://doi.org/10.1007/s13399-021-01850-x.

Mu, R., Liu, B., Chen, X., Wang, N., & Yang, J. (2020). Hydrogel adsorbent in industrial wastewater treatment and ecological environment protection. *Environmental Technology & Innovation*, *20*, 101107. http://doi.org/10.1016/j.eti.2020.101107.

Nascimento, T., Cazarin, C., Maróstica Junior, M., Risso, E., Amaya-Farfan, J., Grimaldi, R., Mercadante, A., Jacob-Lopes, E., & Zepka, L. (2019). Microalgae biomass intake positively modulates serum lipid profile and antioxidant status. *Journal of Functional Foods*, *58*, 11-20. http://doi.org/10.1016/j.jff.2019.04.047.

Nascimento, T., Pinheiro, P., Fernandes, A., Murador, D., Neves, B., Menezes, C., Rosso, V., Jacob-Lopes, E., & Zepka, L. (2021). Bioaccessibility and intestinal uptake of carotenoids from microalgae *Scenedesmus* obliquus. *Lebensmittel-Wissenschaft + Technologie*, *140*, 110780. http://doi.org/10.1016/j.lwt.2020.110780.

Naughton, S., Mathai, M., Hryciw, D., & McAinch, A. (2016). Linoleic acid and the pathogenesis of obesity. *Prostaglandins & Other Lipid Mediators*, *125*, 90-99. http://doi.org/10.1016/j.prostaglandins.2016.06.003. PMid:27350414.

Olsen, M., Pedersen, J., Thomsen, S., Martens, H., Petersen, A., & Jensen, P. (2021). Outdoor cultivation of a novel isolate of the microalgae *Scenedesmus* sp. and the evaluation of its potential as a novel protein crop. *Physiologia Plantarum*, *173*(2), 483-494. http://doi.org/10.1111/ppl.13532. PMid:34427928.

Oreste, E. Q., Jesus, A., Oliveira, R. M., Silva, M. M., Vieira, M. A., & Ribeiro, A. S. (2013). New design of cold finger for sample preparation in open system: Determination of Hg in biological samples by CV-AAS. *Microchemical Journal*, *109*, 5-9. http://doi.org/10.1016/j.microc.2012.05.034.

Pacheco, B., Santos, M., Schultze, E., Martins, R., Lund, R., Seixas, F., Colepicolo, P., Collares, T., Paula, F., & Pereira, C. (2018). Cytotoxic activity of fatty acids from Antarctic macroalgae on the growth of human breast cancer cells. *Frontiers in Bioengineering and Biotechnology*, *6*, 185. http://doi.org/10.3389/fbioe.2018.00185. PMid:30560124.

Papageorgiou, S., Kouvelos, E., Favvas, E., Sapalidis, A., Romanos, G., & Katsaros, F. (2010). Metal-carboxylate interactions in metal-alginate complexes studied with FTIR spectroscopy. *Carbohydrate Research*, *345*(4), 469-473. http://doi.org/10.1016/j.carres.2009.12.010. PMid:20044077.

Patil, L., & Kaliwal, B. B. (2019). Microalga *Scenedesmus* bajacalifornicus BBKLP-07, a new source of bioactive compounds with in vitro pharmacological applications. *Bioprocess and Biosystems Engineering*, *42*(6), 979-994. http://doi.org/10.1007/s00449-019-02099-5. PMid:30847556.

Pauwels, B., Korst, A., de Pooter, C., Pattyn, G., Lambrechts, H., Baay, M., Lardon, F., & Vermorken, J. (2003). Comparison of the sulforhodamine B assay and the clonogenic assay for in vitro chemoradiation studies. *Cancer Chemotherapy and Pharmacology*, *51*(3), 221-226. http://doi.org/10.1007/s00280-002-0557-9. PMid:12655440.

Pawlicka, A., Tavares, F., Dörr, D., Cholant, C., Ely, F., Santos, M., & Avellaneda, C. (2019). Dielectric behavior and FTIR studies of xanthan gum-based solid polymer electrolytes. *Electrochimica Acta*, *305*, 232-239. http://doi.org/10.1016/j.electacta.2019.03.055.

Pedra, N., Bona, N., Aguiar, M., Spohr, L., Alves, F., Santos, F., Saraiva, J., Stefanello, F., Braganhol, E., & Spanevello, R. (2022). Impact of gallic acid on tumor suppression: Modulation of redox homeostasis and purinergic response in in vitro and a preclinical glioblastoma model. *The Journal of Nutritional Biochemistry*, *110*, 109156. http://doi.org/10.1016/j.jnutbio.2022.109156. PMid:36255060.

Pereira, A., Rodrigues, F., Paulino, A., Martins, A., & Fajardo, A. (2021). Recent advances on composite hydrogels designed for the remediation of dye-contaminated water and wastewater: A review. *Journal of Cleaner Production*, *284*, 124703. http://doi.org/10.1016/j.jclepro.2020.124703.

Picoloto, R., Pereira, R., Costa, V., Hartwig, C., Pereira, C., Colepicolo, P., Duarte, F., & Mesko, M. F. (2017). Investigating essential and toxic elements in Antarctic macroalgae using a green analytical method. *Journal of Applied Phycology*, *29*(2), 741-749. http://doi.org/10.1007/s10811-016-1000-7.

Quadrado, R., Macagnan, K., Moreira, A., & Fajardo, A. (2022). Redox-responsive hydrogels of thiolated pectin as vehicles for the smart release of acetaminophen. *Reactive & Functional Polymers*, *181*, 105448. http://doi.org/10.1016/j.reactfunctpolym.2022.105448.

Rizwan, M., Mujtaba, G., Memon, S., Lee, K., & Rashid, N. (2018). Exploring the potential of microalgae for new biotechnology applications and beyond: A review. *Renewable & Sustainable Energy Reviews*, *92*, 394-404. http://doi.org/10.1016/j.rser.2018.04.034.

Rodriguez-Amaya, D. B. (2001). *A guide to carotenoid analysis in foods* (Vol. 71). ILSI press.

Sadeghi, A., Rajabiyan, A., Nabizade, N., Meygolinezhad, N., & Ahmady, A. (2024). Seaweed-derived phenolic compounds as diverse bioactive molecules: A review on identification, application, extraction and purification strategies. *International Journal of Biological Macromolecules*, *266*(Pt 1), 131147. http://doi.org/10.1016/j.ijbiomac.2024.131147. PMid:38537857.

Santa-María, C., López-Enríquez, S., Paz, S., Geniz, I., Reyes-Quiroz, M., Moreno, M., Palomares, F., Sobrino, F., & Alba, G. (2023). Update on anti-inflammatory molecular mechanisms induced by oleic acid. *Nutrients*, *15*(1), 224. http://doi.org/10.3390/nu15010224. PMid:36615882.

Santi, I., Pacheco, B., Venzke, D., Freitag, R., de Almeida, L., Colepicolo, P., Fujii, M., Dias, D., & Pereira, C. (2021). Sterols in red macroalgae from antarctica: Extraction and quantification by Gas Chromatography-Mass spectrometry. *Polar Biology*, *44*(5), 987-995. http://doi.org/10.1007/s00300-021-02853-0.

Santos, M., Colepicolo, P., Pupo, D., Fujii, M., de Pereira, C., & Mesko, M. (2017). Antarctic red macroalgae: A source of polyunsaturated fatty acids. *Journal of Applied Phycology*, *29*(2), 759-767. http://doi.org/10.1007/s10811-016-1034-x.

Santos, M., Freitas, S., Berneira, L., Mansilla, A., Astorga-España, M., Colepicolo, P., & Pereira, C. (2019). Pigment concentration, photosynthetic performance, and fatty acid profile of sub-Antarctic brown macroalgae in different phases of development from the Magellan Region, Chile. *Journal of Applied Phycology*, *31*(4), 2629-2642. http://doi.org/10.1007/s10811-019-01777-x.

Sathasivam, R., Radhakrishnan, R., Hashem, A., & Abd Allah, E. F. (2019). Microalgae metabolites: A rich source for food and medicine. *Saudi Journal of Biological Sciences*, *26*(4), 709-722. http://doi.org/10.1016/j.sjbs.2017.11.003. PMid:31048995.

Shetty, V., & Sibi, G. (2015). Relationship between total phenolics content and antioxidant activities of microalgae under autotrophic, heterotrophic and mixotrophic growth. *Journal*

of Food Resource Science, *4*(1), 1-9. http://doi.org/10.3923/jfrs.2015.1.9.

Singh, R., Yadav, P., Kumar, A., Hashem, A., Al-Arjani, A., Abd Allah, E. F., Rodríguez Dorantes, A., & Gupta, R. K. (2022). Physiological and biochemical responses of bicarbonate supplementation on biomass and lipid content of green algae *Scenedesmus* sp. BHU1 isolated from wastewater for renewable biofuel feedstock. *Frontiers in Microbiology*, *13*, 839800. http://doi.org/10.3389/fmicb.2022.839800. PMid:35444634.

Singleton, V., Orthofer, R., & Lamuela-Raventós, R. (1999). Analysis of total phenols and other oxidation substrates and antioxidants by means of folin-ciocalteu reagent. In: Packer (Ed.), *Oxidants and Antioxidants Part A* (Methods in Enzymology Book Series, Vol. 299, pp. 152-178). Academic Press. http://doi.org/10.1016/S0076-6879(99)99017-1.

Soltani, N., Latifi, A., Alnajar, N., Dezfulian, M., Shokarvi, S., Heydari, M., & Choopani, A. (2016). Biochemical and physiological characterization of tree microalgae spp. as candidates for food supplement. *Journal of Applied Biotechnology Reports*, 3(1), 377-381.

Souza, R., Saldanha-Corrêa, F., Gallego, A., & Neto, A. (2020). Semi-quantitative determination of ash element content for freeze-dried, defatted, sulfated and pyrolysed biomass of *Scenedesmus* sp. *Biotechnology for Biofuels*, *13*(1), 63. http://doi.org/10.1186/s13068-020-01699-8. PMid:32266009.

Udayan, A., Arumugam, M., & Pandey, A. (2017). Nutraceuticals from algae and cyanobacteria. In: ajesh P. Rastogi, D. Madamwar & A. Pandey (Eds.), *Algal green chemistry: Recent progress in biotechnology* (pp. 65-89). Elsevier. http://doi.org/10.1016/B978-0-444-63784-0.00004-7.

Uribe, E., Pardo-Orellana, C., Vega-Gálvez, A., Ah-Hen, K., Pastén, A., García, V., & Aubourg, S. (2019). Effect of drying methods on bioactive compounds, nutritional, antioxidant, and antidiabetic potential of brown alga *Durvillaea antarctica*. *Drying Technology*, *38*(14), 1915-1928. http://doi.org/10.1080/07373937.2019.1679830.

van Rooijen, M., & Mensink, R. (2020). Palmitic acid versus stearic acid: Effects of interesterification and intakes on cardiometabolic risk markers: a systematic review. *Nutrients*, *12*(3), 615. http://doi.org/10.3390/nu12030615. PMid:32111040.

Waqar, R., Kaleem, M., Iqbal, J., Minhas, L., Haris, M., Chalgham, W., Ahmad, A., & Mumtaz, A. (2023). Kinetic and equilibrium studies on the adsorption of Lead and Cadmium from aqueous solution using *Scenedesmus* sp. *Sustainability (Basel)*, *15*(7), 6024. http://doi.org/10.3390/su15076024.

Wrzosek, M., Zawadzka, Z., Sawicka, A., Bobrowska-Korczak, B., & Białek, A. (2022). Impact of fatty acids on obesity-associated diseases and radical weight reduction. *Obesity Surgery*, *32*(2), 428. http://doi.org/10.1007/s11695-021-05789-w. PMid:34813039.

Zhang, Y., Kong, X., Wang, Z., Sun, Y., Zhu, S., Li, L., & Lv, P. (2018). Optimization of enzymatic hydrolysis for effective lipid extraction from microalgae *Scenedesmus* sp. *Renewable Energy*, *124*, 1049-1057. http://doi.org/10.1016/j.renene.2018.01.078.

Zheng, L., Seidi, F., Wu, W., Pan, Y., & Xiao, H. (2023). Dual-functional lignin-based hydrogels for sustained release of agrochemicals and heavy metal ion complexation. *International Journal of Biological Macromolecules*, *235*, 123701. http://doi.org/10.1016/j.ijbiomac.2023.123701. PMid:36801277.